High-spin states in odd-mass $^{113-119}$Sb: $\Delta J = 1$ bands on $9/2^+$ proton-hole states

R. E. Shroy,* A. K. Gaigalas,† G. Schatz,‡ and D. B. Fossan
Department of Physics, State University of New York, Stony Brook, New York 11794
(Received 26 July 1978)

Properties of high-spin states in ^{113,115,117,119}Sb have been studied via the ^{A}Cd(^{6}Li,$3n$)$^{A+3}$Sb reactions. Using Ge(Li) and Si(Li) detectors, in-beam measurements of γ-ray excitation functions, γ-γ coincidences, γ-ray angular distributions, and pulsed beam-γ timing spectra were made to determine level energies, decay schemes, γ-ray multipolarities, J^π assignments, isomeric lifetimes, and a g factor. Systematic $\Delta J = 1$ bands built on low-lying $9/2^+$ proton-hole (2p-1h) states were observed in these nuclei. The bandheads that involve the excitation of a $1g_{9/2}$ proton across the $Z = 50$ shell achieve an energy minimum near the middle of the neutron shell. The observed properties of these bands are consistent with significant prolate deformations; the band spacings imply a deformation asymmetry of $\gamma = 20^\circ$ in a triaxial rotor model. In addition, single-particle and single-particle plus core-excitation states were observed in these Sb nuclei. Two isomers were identified, a $19/2^{(-)}$ state at 2796 keV in ^{115}Sb ($\tau = 230 \pm 4$ ns and $g = +0.290 \pm 0.005$) and a $(27/2^+)$ state in ^{119}Sb ($\tau = 1.23 \pm 0.13$ s).

[NUCLEAR REACTIONS $^{110-116}$Cd(^{6}Li, $3n$)$^{113-119}$Sb; measured γ-γ coincidences, $\gamma(E,\theta,t)$, spin rotation in $B = 10.3$ kG; deduced level schemes in odd-mass $^{113-119}$Sb, γ multipolarities, J^π, $T_{1/2}$, g-factor. Enriched targets, Ge(Li) detectors.]

I. INTRODUCTION

The nuclear structure of the odd-mass Sb isotopes ($Z = 51$) is expected to be understandable in simple theoretical terms because of the $Z = 50$ shell closure. Previous experiments have determined much of the low-spin structure of these nuclei[1-11] and reasonable success has been achieved in their theoretical treatment.[12,13] The theory has involved an odd proton, in the available spherical shell-model orbitals ($2d_{5/2}$, $1g_{7/2}$, $3s_{1/2}$, $2d_{3/2}$, $1h_{11/2}$), coupled to phonon excitations of the Sn core. To further test the theoretical understanding, it is desirable to extend the experimental information to the high-spin states. The observation of high-spin states that correspond to an odd proton coupled to phonon excitations would help to complete the determination of the proton-phonon coupling. High-spin states that correspond to an odd proton coupled to a specific broken neutron pair in high-j orbitals are also expected.

The study of high-spin states in odd-mass Sb nuclei also provides information on deformed states which coexist with these spherical states. In an earlier publication[14] covering a portion of the present study, a sequence of $\Delta J = 1$ bands built on low-lying $\frac{9}{2}^+$ proton-hole states in the ^{113,115,117,119}Sb nuclei was reported. These $\frac{9}{2}^+$ bandheads are believed to result from the excitation of a $1g_{9/2}$ proton across the $Z = 50$ closed shell. The low energies and the rotationlike band spacings suggest a large deformation. The two particle-one hole (2p-1h) structure has also been implied by $L = 4$ Te(t,α) pickup strength[4] to some of these states. Successful calculations in terms of a $[404]\frac{9}{2}^+$ Nilsson proton-hole orbital and appropriate potential energy surfaces for the two-proton prolate cores have been made for these $\frac{9}{2}^+$ states.[15,16] Results from a previous ($\alpha,2n$) experiment[17] had determined part of the $\Delta J = 1$ band in ^{117}Sb for which a deformed rotor interpretation was given. Recently, several other light-ion studies have been made which yield information on high-spin states in several Sb isotopes.[18,19,7]

In this paper the complete experimental results of our study of high-spin states in ^{113,115,117,119}Sb, for which preliminary reports[20] have been given, are presented including several recent lifetime and g-factor measurements. This work is part of a larger study of high-spin states in odd-mass Sb($Z = 51$),[21] I($Z = 53$),[22,23] Cs($Z = 55$),[24] and La($Z = 57$)[25] nuclei. The collective properties extracted from this larger study[26] for the $Z \gtrsim 50$ region have been approached theoretically from both the particle-rotor[27-30] and particle-vibrator[31-33] descriptions.

In the present work, the odd-mass Sb nuclei were populated via the (^{6}Li, $3n$) fusion-evaporation reaction with even Cd targets; this reaction allows a systematic investigation of these nuclei because several of the even Cd isotopes are stable. The high-spin states, which are selectively populated by these reactions, were studied by the following in-beam γ-ray measurements: (1) γ-ray excitation measurements, (2) γ-γ coincidence measurements, (3) γ-ray angular distribution measurements, (4) pulsed beam-γ

measurements, and (5) γ-ray perturbed angular distribution measurements. The experimental techniques involved in these measurements are discussed in Sec. II of this paper.

The experimental results extracted from the above measurements, include excitation energies, J^{π} assignments, lifetimes, and electromagnetic moments for the high-spin states. This information is given in Sec. III for each of the odd-mass Sb isotopes studied. Section IV contains a discussion of the theoretical interpretation of these experimental results.

II. EXPERIMENTAL TECHNIQUES

The ^{113,115,117,119}Sb nuclei studied in this project were produced by the (^{6}Li, $3n$) reaction with a ^{6}Li beam from the Stony Brook Fn tandem Van de Graaff accelerator. Like other (HI, xn) fusion-evaporation reactions[34] the (^{6}Li, $3n$) reaction preferentially populates high-spin states; orbital angular momentum transfers as large as $17\hbar$ can be achieved with 34 MeV ^{6}Li. Further, the dominant γ-ray decay mode of the residual nucleus is through yrast states, those states of a given angular momentum which lie lowest in energy. The targets used in most of the experiments were ~10 mg/cm^2 (~3 MeV thick for 34 MeV ^{6}Li) enriched metallic foils of ^{110,112,114,116}Cd. In these studies, γ rays were observed with one or two large volume Ge(Li) detectors which had typical energy resolutions (FWHM) of 2.5 keV at 1.33 MeV. Also a 5 mm thick planar intrinsic Ge detector which had a resolution (FWHM) of 0.5 keV at 122 keV was used for low energy γ rays.

The experimental measurements that are commonly employed to determine level structures and decay properties via (HI, xn) reactions have previously been discussed in detail.[35] In the following sections the essential aspects of the measurements performed in this study will be given.

A. γ-ray excitation measurements

The intensity of each γ ray was measured as a function of excitation energy by varying the energy of the ^{6}Li beam from 24 to 34 MeV. These excitation measurements are helpful in identifying γ rays from a given residual nucleus because the cross sections for different channels populated by fusion-evaporation reactions peak at different, well-separated energies. The excitation measurements were also used to choose the optimal beam energy at which to perform the various measurements. The cross section for a (HI, xn) reaction is approximately described by a peak (~10 MeV wide) with a centroid given by $E_{pk} = (1 + M_B/M_T) \times (-Q + 6x)$ MeV,[34] where M_B and M_T are the masses of the beam and target nuclei, Q is the Q value of the reaction, and x is the number of evaporated neutrons. The separation of $E_{pk}(x)$ from $E_{pk}(x \pm 1)$ is of the order of 14 MeV. A ^{6}Li energy of 34 MeV was chosen for the measurements of each target as a compromise between the predicted optimal energy and beam energy limitations. Singles spectra taken at this energy are shown in Fig. 1 for all four targets.

B. γ-γ coincidence measurements

In order to identify γ rays from the nucleus of interest and to locate the γ-ray cascades in a decay scheme, γ-γ coincidence measurements were performed. These measurements were made both with Ge(Li) detectors, and with a Ge(Li) and an intrinsic Ge detector. Using standard fast-slow timing, information consisting of the energies of two γ rays and the time difference between them were written on magnetic tape in an event-by-event mode. Time differences of up to ±500 ns were accepted. For each target more than 10^7 such events were collected for analysis after the experiment. In this analysis, coincident energy spectra were scanned for each full energy peak and an appropriate time region. Compton background was subtracted using coincidence spectra collected for regions near the full energy peaks. Random coincidences were found to be negligible. Several typical γ-γ coincidence spectra for γ rays in ^{119}Sb are shown in Fig. 2. The results of all γ-γ coincidence gates have been listed in tabular form[36] for γ rays assigned to ^{113,115,117,119}Sb.

C. Angular distribution measurements

Intensities and anisotropies of the γ rays were obtained from angular distribution measurements. The intensities were needed to order transitions within a cascade and to determine branching ratios, while the anisotropies were used in the determination of γ-ray multipolarities and in the assignment of spin values. In these experiments, the relative intensity of each γ ray was measured with a Ge(Li) detector at four angles between 27° and 90° for ^{113,117,119}Sb and at five angles between 0° and 90° for ^{115}Sb. The observed angular distributions were then fitted to the expression $I(\theta) = I_\gamma[1 + A_2 P_2(\cos\theta) + A_4 P_4(\cos\theta)]$, where P_k is a Legendre polynomial, and I_γ is the γ-ray intensity. The fits were performed both with the A_4 fixed at zero and with A_4 allowed to vary; for A_k values consistent with a pure dipole transition, the quoted value of A_2 is that obtained from the fit with $A_4 = 0$. The intensities I_γ, corrected for detector efficiency, and the A_2 and A_4 values derived from the angular distributions are listed in Table I

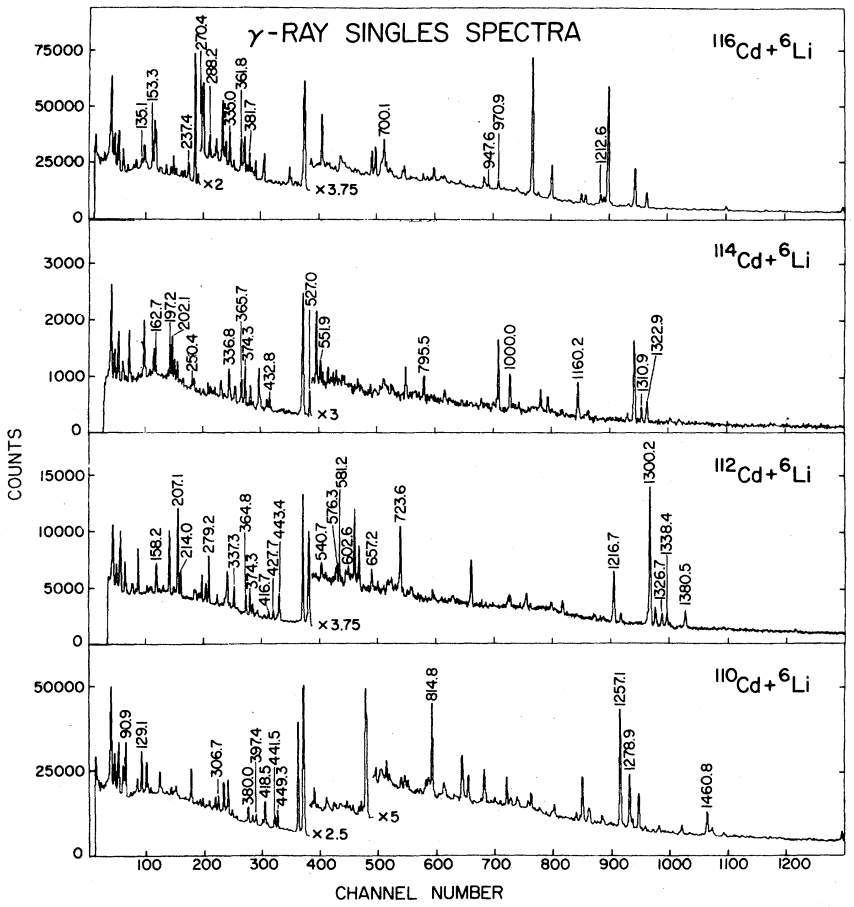

FIG. 1. The γ-ray singles spectra observed with a Ge(Li) detector for the bombardment of ^{110,112,114,116}Cd targets with a 34-MeV ^{6}Li beam. The γ-ray energies are in keV.

for the γ rays of interest. Typical angular distribution data and fits are shown in Fig. 3 for several transitions in ^{115}Sb.

Spin assignments (multipolarities) deduced from the A_k values are given in Table I. Mixing ratios extracted for transitions whose A_k values could be accurately determined are also given in this table.

The spin assignments given here were obtained by using transition-multipolarity information obtained from the angular distribution data together with previously known spins of low-lying states. Previous studies of heavy-ion fusion-evaporation reactions have shown two important properties: (1) The preferentially populated high-spin states are aligned in low-m substates since the orbital angular momentum brought into the compound nucleus is perpendicular to the beam direction, and (2) these states decay predominantly by stretched $J \rightarrow J - L$ γ-ray transitions of multipolarity L, although competition from the $L+1$ multipolarity in the case of parity-unfavored transitions may also occur. To extract the multipolarity and mixing ratio information, the experimental A_k values were compared with values calculated assuming these two properties. In these calculations the m-substate population was taken to be a Gaussian distribution $P(m) = (1/N)\exp[-m^2/(2\sigma^2)]$, where $P(m)$ is the probability of populating a given m substate, N is a normalization constant, and σ is the width of the Gaussian. The same value of σ can be applied to states of similar energy and spin. Values of σ, which were extracted from the angular distributions of γ rays known to originate from stretched transitions of a pure multipolarity, are listed in Table I. An average value of $\sigma = 2.2 \pm 0.3$ was obtained, in agreement with that from a previous (^{6}Li, $3n$) study[35] at 34 MeV. Lifetimes and lifetime limits were also useful in making spin assignments because such information can exclude the presence of higher multipolarities in a decay transition. The spin assignment made in this way are not always completely rigorous due to the assumptions concerning the m-substate population and stretched γ-ray transitions; however, the spin assignments presented here are considered to be strong because these assumptions have been found to be empirically valid for dominant transitions

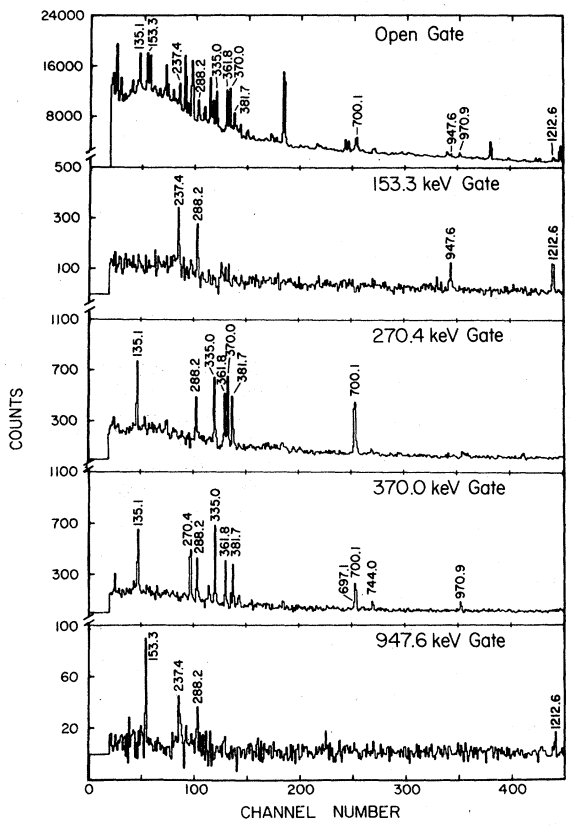

FIG. 2. Representative γ-γ coincidence spectra from the ^{116}Cd(^{6}Li, $3n$)^{119}Sb reaction for selected γ-ray gates.

in such heavy-ion reactions and because the assumptions have a sound theoretical basis.

In extracting the multipolarity information and mixing ratios, it was necessary to take into account the effects of cascade feeding from isomeric states. The isomeric states may live long enough to have their alignment reduced due to interactions with hyperfine fields in the target. In the present study, a negligible alignment was found for several Sb isomers with $\tau > 200$ ns, consistent with isotropic γ rays for the direct decay transitions of these isomers.

D. Pulsed beam-γ measurements

Pulsed beam-γ timing studies on all four targets were performed to search for isomeric states and to measure lifetimes or lifetime limits. Besides determining transition strengths, lifetime information was used to exclude the existence of high multipolarities in decay transitions. Using pulsed ^{6}Li beams of 1 and 4 μs repetition periods with pulse widths of ~2 ns (FWHM), the energies and associated time delays relative to the beam pulse were measured for all γ rays using a Ge(Li) detector. An overall time resolution of ~8 ns (FWHM) was obtained with the Ge(Li) detector. In these studies, the data for all four targets were taken in two ways. First, γ-ray energy spectra were collected for several time regions between pulses; this method allowed identification of all delayed γ rays and yielded approximate lifetime information. Secondly, time spectra were collected time differentially for selected γ rays to obtain precise lifetimes for specific isomers. In order to measure the lifetime of a long-lived isomer discovered in ^{119}Sb, a mechanical wheel was used to pulse the ^{6}Li beam at a repetition period of 3 s and a 40% duty cycle.

E. Perturbed angular distributions

After pulsed beam studies revealed a $\tau = 230$ ns isomer in ^{115}Sb, this isomeric state was further investigated with a measurement of its g factor. The method used was the Time Differential Perturbed Angular Distribution (TDPAD) method. In this method the isomer is excited by the beam pulse after which the γ-ray angular distribution is observed to precess as a function of time in an external magnetic field. The magnetic field strength was calibrated to be 10.3 kG by a measurement of the known g factor[37] of the $\frac{9}{2}^{+}$ state in ^{69}Ge. A thick 60 mg/cm^2 ^{112}Cd target, which stopped the beam, was used for this g-factor measurement. The 1217-keV delayed γ ray in ^{115}Sb was observed with NaI detectors at $\pm 135°$ with respect to the beam direction. The resulting time spectra were evaluated by forming the usual ratio,

$$R(t) = \frac{I(-135°, t) - I(135°, t)}{I(-135°, t) + I(135°, t)} ,$$

where $I(\theta, t)$ is the γ-ray intensity at an angle θ and a time t relative to the beam pulse. The ratio spectra were fitted to the function

$$R(t) = [3A_2/(4+A_2)] \sin(2\omega_L t + \phi) ,$$

where $\omega_L = -g\mu_n H/\hbar$ is the Larmor precession frequency and ϕ is a phase shift which allows for angular deviations such as beam bending in the magnetic field. In this expression, terms in A_4 have been neglected since A_4 is small and because the ratio function is only weakly dependent on A_4. In order to eliminate the loss of nuclear alignment caused by radiation-induced lattice damage, it was necessary to heat the target to 510 °K. This loss of alignment, which was studied carefully for Sb in Cd as a function of temperature, has been reported.[38]

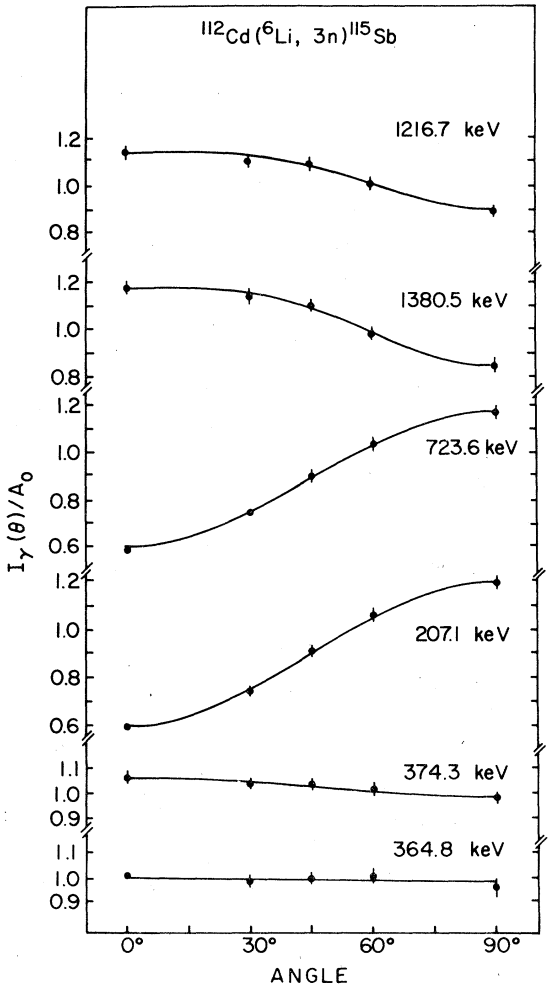

FIG. 3. The angular distributions of intensities measured for representative γ rays from the ^{112}Cd(^{6}Li, 3n) ^{115}Sb reaction.

III. EXPERIMENTAL RESULTS FOR ^{113,115,117,119}Sb

The singles γ-ray spectra produced by the 34 MeV ^{6}Li beam on the Cd targets were found to be complicated, containing products from several residual nuclei. Analysis showed that (^{6}Li, 3n) was the dominant fusion-evaporated reaction at this energy, accounting for 50–60% of the total cross section. Even Sn nuclei, which are populated by (^{6}Li, $p3n$) and possibly by ^{6}Li breakup into an α particle and a deuteron followed by (α, 2n), were the second largest residual product with 15–20% of the total cross section in each case. The (^{6}Li, $p2n$) reaction to the odd Sn nuclei had ~20% of the cross section for the ^{110}Cd target, but this reaction decreased for heavier targets to < 5% for ^{116}Cd. Other reactions observed weakly (< 5%) were the (^{6}Li, 2n), (^{6}Li, 4n), and ^{6}Li breakup fol-

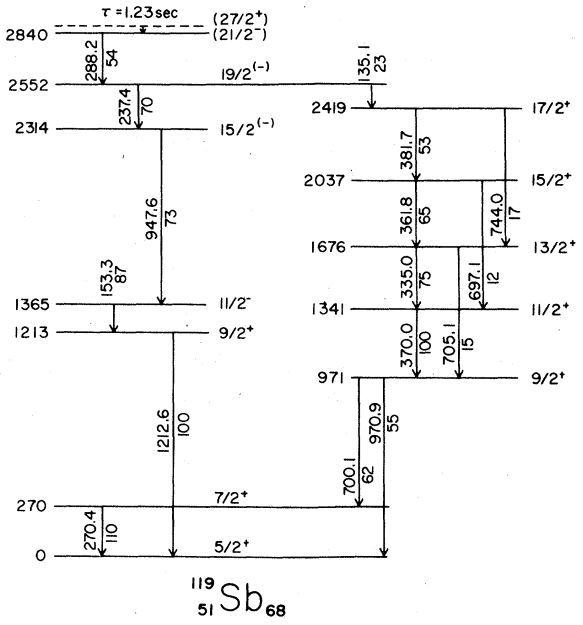

FIG. 4. The level structure and decay scheme of ^{119}Sb determined in the present study. The γ-ray energies (keV) and intensities, relative to the $\frac{11}{2}^{+} \rightarrow \frac{9}{2}^{+}$ transition, are listed by each γ-ray arrow.

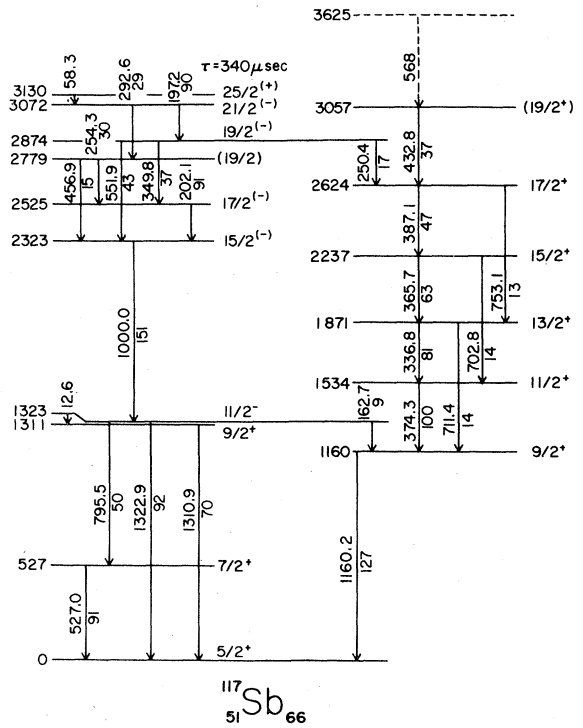

FIG. 5. The level structure and decay scheme of ^{117}Sb determined in the present study.

TABLE I. Experimental results of angular distribution measurements for ^{113,115,117,119}Sb.

E_γ (keV) [a]	I_γ [b]	A_2	A_4	$J_i^\pi \rightarrow J_f^\pi$	B.R. (%) [c]	Other [d]
			^{119}Sb			
135.1 ± 0.5	23 ± 3	−0.03 ± 0.03		$\frac{19}{2}^{(-)} \rightarrow \frac{17}{2}^{+}$	25 ± 4	δ = 0.11 ± 0.03
153.3 ± 0.5	87	−0.10 ± 0.04		$\frac{11}{2}^{-} \rightarrow \frac{9}{2}^{+}$		δ = 0.02 ± 0.05
237.4 ± 0.3	70	0.14 ± 0.05	−0.03 ± 0.06	$\frac{19}{2}^{(-)} \rightarrow \frac{15}{2}^{(-)}$	75 ± 4	δ = −0.06 ± 0.09
270.4 ± 0.4	110	−0.15 ± 0.03	0.01 ± 0.04	$\frac{7}{2}^{+} \rightarrow \frac{5}{2}^{+}$		δ = −0.04 ± 0.04
288.2	54	−0.04 ± 0.04	−0.02 ± 0.04	$(\frac{21}{2}^{-}) \rightarrow \frac{19}{2}^{(-)}$		δ = 0.51 ± 0.50
335.0	75	0.06 ± 0.04	0.04 ± 0.05	$\frac{13}{2}^{+} \rightarrow \frac{11}{2}^{+}$	84 ± 5	δ = 0.20 ± 0.04
361.8 ± 0.5	65	0.06 ± 0.04	0.02 ± 0.04	$\frac{15}{2}^{+} \rightarrow \frac{13}{2}^{+}$	85 ± 6	δ = 0.19 ± 0.08
370.0	100	0.15 ± 0.04	0.03 ± 0.05	$\frac{11}{2}^{+} \rightarrow \frac{9}{2}^{+}$		δ = 0.30 ± 0.05
381.7	53	0.00 ± 0.05	0.02 ±0.05	$\frac{17}{2}^{+} \rightarrow \frac{15}{2}^{+}$	74 ± 8	δ = 0.15 ± 0.05
697.1 ± 0.5	12 ± 3	0.27 ± 0.11	0.02 ± 0.11	$\frac{15}{2}^{+} \rightarrow \frac{11}{2}^{+}$	15 ± 6	δ = −0.03 ± 0.09
700.1 ± 0.5	62	−0.23 ± 0.04	0.07 ± 0.06	$\frac{9}{2}^{+} \rightarrow \frac{7}{2}^{+}$	53 ± 3	δ = −0.09 ± 0.07
705.1 ± 0.5	15 ± 3	0.18 ± 0.09	−0.10 ± 0.11	$\frac{13}{2}^{+} \rightarrow \frac{9}{2}^{+}$	16 ± 5	δ = −0.12 ±0.14
744.0 ± 0.5	17 ± 3			$\frac{17}{2}^{+} \rightarrow \frac{13}{2}^{+}$	26 ± 8	
947.6 ± 0.5	73	0.15 ± 0.07	−0.12 ± 0.10	$\frac{15}{2}^{(-)} \rightarrow \frac{11}{2}^{-}$		δ = −0.03 ± 0.20
970.9 ± 0.5	55	0.26 ± 0.06	−0.03 ± 0.05	$\frac{9}{2}^{+} \rightarrow \frac{5}{2}^{+}$	47 ± 3	σ = 1.9 ± 0.4
1212.6 ± 0.5	100	0.18 ± 0.04	−0.03 ± 0.10	$\frac{9}{2}^{+} \rightarrow \frac{5}{2}^{+}$		σ = 2.0 ± 0.3
			^{117}Sb			
12.6 ± 0.2				$\frac{11}{2}^{-} \rightarrow \frac{9}{2}^{+}$		
58.3 ± 0.2				$\frac{25}{2}^{(+)} \rightarrow \frac{21}{2}^{(-)}$		
162.7	9 ± 2	−0.11 ± 0.05		$\frac{11}{2}^{-} \rightarrow \frac{9}{2}^{+}$	6 ± 2	σ = 2.1 ± 1.0
197.2	90 ± 10	−0.10 ± 0.03	0.01 ± 0.04	$\frac{21}{2}^{(-)} \rightarrow \frac{19}{2}^{(-)}$	72 ± 6	δ = −0.10 ± 0.06
202.1	91	−0.11 ± 0.04	0.02 ± 0.04	$\frac{17}{2}^{(-)} \rightarrow \frac{15}{2}^{(-)}$		δ = 0.03 ± 0.05
250.4	17 ± 2	−0.02 ± 0.06		$\frac{19}{2}^{(-)} \rightarrow \frac{17}{2}^{+}$	19 ± 4	
254.3 ± 0.5	30	−0.10 ± 0.05	0.03 ± 0.06	$\frac{19}{2} \rightarrow \frac{17}{2}^{(-)}$	69 ± 4	δ = 0.03 ± 0.08
292.6 ± 0.5	29	0.04 ± 0.06	−0.01 ± 0.08	$\frac{21}{2}^{(-)} \rightarrow (\frac{19}{2})$	28 ± 6	δ = 0.25 ± 0.31
349.8 ± 0.5	37	−0.06 ± 0.05	−0.09 ± 0.08	$\frac{19}{2}^{(-)} \rightarrow \frac{17}{2}^{(-)}$	38 ± 4	δ = 0.02 ± 0.08
336.8	81	−0.01 ± 0.04	−0.01 ± 0.05	$\frac{13}{2}^{+} \rightarrow \frac{11}{2}^{+}$	86 ± 5	δ = 0.15 ± 0.05
365.7	63	−0.06 ± 0.04	0.04 ± 0.05	$\frac{15}{2}^{+} \rightarrow \frac{13}{2}^{+}$	81 ± 6	δ = 0.10 ± 0.05
374.3	100	0.08 ± 0.04	0.06 ± 0.05	$\frac{11}{2}^{+} \rightarrow \frac{9}{2}^{+}$		δ = 0.23 ± 0.05
387.1 ± 0.5	47	−0.02 ± 0.10	0.09 ± 0.06	$\frac{17}{2}^{+} \rightarrow \frac{15}{2}^{+}$	75 ± 6	δ = 0.16 ± 0.09
432.8 ± 0.5	37			$(\frac{19}{2}^{+}) \rightarrow \frac{17}{2}^{+}$		
456.9 ± 0.5	15 ± 2	0.15 ± 0.06	−0.07 ± 0.06	$\frac{19}{2} \rightarrow \frac{15}{2}^{(-)}$	31 ± 4	δ = −0.06 ± 0.20
527.0	91	−0.26 ± 0.04	0.06 ± 0.04	$\frac{7}{2}^{+} \rightarrow \frac{5}{2}^{+}$		δ = −0.37 ± 0.06
551.9	43	0.03 ± 0.05	0.02 ± 0.08	$\frac{19}{2}^{(-)} \rightarrow \frac{15}{2}^{(-)}$	43 ± 4	δ = −0.24 ± 0.27
568.0 ± 1.0						
702.8 ± 0.5	14 ± 3			$\frac{15}{2}^{+} \rightarrow \frac{11}{2}^{+}$	19 ± 6	
711.4 ± 0.5	14 ± 3	0.15 ± 0.09	−0.08 ± 0.10	$\frac{13}{2}^{+} \rightarrow \frac{9}{2}^{+}$	14 ± 5	δ = −0.16 ± 0.19
753.1 ± 0.5	13 ± 3			$\frac{17}{2}^{+} \rightarrow \frac{13}{2}^{+}$	25 ± 6	
795.5 ± 0.4	50	0.18 ± 0.05	−0.02 ± 0.04	$\frac{11}{2}^{-} \rightarrow \frac{7}{2}^{+}$	33 ± 4	δ = 0.05 ± 0.20
1000.0 ± 0.5	151	0.10 ± 0.04	−0.06 ± 0.05	$\frac{15}{2}^{(-)} \rightarrow \frac{11}{2}^{-}$		σ = 2.8 ± 0.6
1160.2 ± 0.4	127	0.16 ± 0.04	−0.04 ± 0.05	$\frac{9}{2}^{+} \rightarrow \frac{5}{2}^{+}$		σ = 2.5 ± 0.4

TABLE I. (*Continued*)

E_γ (keV) [a]	I_γ [b]	A_2	A_4	$J_i^\pi \rightarrow J_f^\pi$	B.R. (%) [c]	Other [d]
1310.9 ± 0.4	70	0.15 ± 0.05	−0.06 ± 0.07	$\frac{9}{2}^+ \rightarrow \frac{5}{2}^+$		σ = 2.4 ± 0.4
1322.9 ± 0.5	92	0.27 ± 0.04	0.06 ± 0.04	$\frac{11}{2}^- \rightarrow \frac{5}{2}^+$	61 ± 4	σ = 2.1 ± 0.4
			^{115}Sb			
158.2 ± 0.2	35 ± 4	0.02 ± 0.04	−0.07 ± 0.06	$\frac{19}{2}^{(-)} \rightarrow \frac{15}{2}^{(-)}$	24 ± 4	δ = −0.08 ± 0.09
207.1 ± 0.2	140	−0.40 ± 0.03	0.00 ± 0.04	$\frac{21}{2}^{(-)} \rightarrow \frac{19}{2}^{(-)}$		δ = −0.08 ± 0.06
214.0	40	−0.23 ± 0.04	−0.02 ± 0.04	$\frac{25}{2}^{(+)} \rightarrow \frac{23}{2}^{(-)}$		δ = −0.01 ± 0.05
279.2	108	0.04 ± 0.05	−0.05 ± 0.06	$\frac{19}{2}^{(-)} \rightarrow \frac{15}{2}^{(-)}$	76 ± 4	
337.3	83	0.02 ± 0.04	−0.03 ± 0.04	$\frac{13}{2}^+ \rightarrow \frac{11}{2}^+$	81 ± 5	δ = 0.17 ± 0.05
364.8	62	0.00 ± 0.04	−0.01 ± 0.05	$\frac{15}{2}^+ \rightarrow \frac{13}{2}^+$	82 ± 6	δ = 0.15 ± 0.04
374.3	100	0.06 ± 0.04	−0.01 ± 0.03	$\frac{11}{2}^+ \rightarrow \frac{9}{2}^+$	76 ± 5	δ = 0.21 ± 0.04
380.6	38	−0.01 ± 0.05	0.03 ± 0.04	$\frac{17}{2}^+ \rightarrow \frac{15}{2}^+$	74 ± 6	δ = 0.14 ± 0.05
416.7 ± 0.5	21	0.05 ± 0.05	−0.05 ± 0.06	$\frac{19}{2}^+ \rightarrow \frac{17}{2}^+$	69 ± 8	δ = 0.18 ± 0.06
427.7 ± 0.5	32	0.16 ± 0.05	0.05 ± 0.05	$\frac{11}{2}^+ \rightarrow \frac{9}{2}^+$	24 ± 5	δ = 0.28 ± 0.06
437.2 ± 0.5	16 ± 2	−0.02 ± 0.06	0.07 ± 0.05	$\frac{21}{2}^+ \rightarrow \frac{19}{2}^+$	76 ± 8	δ = 0.13 ± 0.05
441.6 ± 0.5	47	−0.71 ± 0.03	0.00 ± 0.05	$\frac{23}{2}^{(-)} \rightarrow \frac{21}{2}^{(-)}$		δ = −0.28 ± 0.06
443.4 ± 0.5	32	0.36 ± 0.04	−0.12 ± 0.08	$\frac{23}{2} \rightarrow \frac{19}{2}$	64 ± 6	δ = 0.00 ± 0.06
540.7 ± 0.5	16 ± 2			$\frac{23}{2} \rightarrow \frac{21}{2}^{(-)}$	36 ± 6	
576.3 ± 0.5	28	0.11 ± 0.06	−0.09 ± 0.10	$\frac{11}{2}^- \rightarrow \frac{7}{2}^+$		
581.2 ± 0.4	35	0.10 ± 0.05	−0.03 ± 0.05	$\frac{19}{2} \rightarrow \frac{15}{2}^{(-)}$		δ = −0.23 ± 0.06
602.6 ± 0.4	35	−0.22 ± 0.05	0.02 ± 0.06	$\frac{9}{2}^+ \rightarrow \frac{7}{2}^+$	32 ± 5	δ = −0.05 ± 0.08
657.2	35	−0.24 ± 0.04	0.00 ± 0.06	$\frac{9}{2}^+ \rightarrow \frac{7}{2}^+$	29 ± 5	δ = −0.07 ± 0.07
702.1 ± 0.4	14 ± 3			$\frac{15}{2}^+ \rightarrow \frac{11}{2}^+$	18 ± 6	
709.1 ± 0.4	16 ± 3	0.17 ± 0.08	−0.03 ± 0.09	$\frac{13}{2}^+ \rightarrow \frac{9}{2}^+$	19 ± 5	δ = −0.16 ± 0.20
723.6	164	−0.37 ± 0.04	−0.02 ± 0.05	$\frac{7}{2}^+ \rightarrow \frac{5}{2}^+$		
746.3 ± 0.4	13 ± 3			$\frac{17}{2}^+ \rightarrow \frac{13}{2}^+$	26 ± 6	
797.8 ± 0.5	10 ± 3			$\frac{19}{2}^+ \rightarrow \frac{15}{2}^+$	31 ± 8	
853.3 ± 0.5	6 ± 2			$\frac{21}{2}^+ \rightarrow \frac{17}{2}^+$	24 ± 8	
1216.7 ± 0.5	145	0.08 ± 0.05	−0.06 ± 0.05	$\frac{15}{2}^{(-)} \rightarrow \frac{11}{2}^-$		δ = −0.04 ± 0.07
1300.2 ± 1.0				$\frac{11}{2}^- \rightarrow \frac{5}{2}^+$		
1326.8 ± 0.5	81	0.21 ± 0.05	−0.05 ± 0.05	$\frac{9}{2}^+ \rightarrow \frac{5}{2}^+$	68 ± 5	δ = −0.05 ± 0.09
1338.4 ± 0.5	60	0.13 ± 0.04	−0.08 ± 0.06	$\frac{15}{2}^{(-)} \rightarrow \frac{11}{2}^-$		δ = −0.04 ± 0.08
1380.5 ± 0.5	100	0.25 ± 0.04	−0.07 ± 0.05	$\frac{9}{2}^+ \rightarrow \frac{5}{2}^+$	71 ± 5	δ = 0.02 ± 0.09
			^{113}Sb			
90.9 ± 0.2	172 ± 18	−0.19 ± 0.04		$\frac{11}{2}^- \rightarrow \frac{9}{2}^+$	81 ± 6	δ = 0.01 ± 0.05
129.1 ± 0.2	122 ± 13	−0.42 ± 0.04	0.02 ± 0.07	$\frac{21}{2}^{(-)} \rightarrow \frac{19}{2}^{(-)}$		δ = −0.10 ± 0.04
197.1	18 ± 2	−0.09 ± 0.09	0.10 ± 0.11	$(\frac{15}{2}^+) \rightarrow (\frac{13}{2}^+)$	33 ± 6	δ = 0.09 ± 0.06
287.2	38	−0.11 ± 0.07	0.07 ± 0.12	$(\frac{15}{2}^+) \rightarrow \frac{13}{2}^+$	67 ± 6	δ = 0.08 ± 0.09
306.7 ± 0.5	50	0.02 ± 0.05	0.04 ± 0.16	$\frac{13}{2}^+ \rightarrow \frac{11}{2}^+$	60 ± 5	δ = 0.16 ± 0.06
351.5 ± 0.4	12 ± 2			$\frac{15}{2} \rightarrow (\frac{13}{2}^+)$	18 ± 4	

TABLE I. (*Continued*)

E_γ (keV) [a]	I_γ [b]	A_2	A_4	$J_i^\pi \rightarrow J_f^\pi$	B.R. (%) [c]	Other [d]
380.0 ± 0.4	60	−0.67 ± 0.04	−0.01 ± 0.05	$\frac{23}{2}^{(-)} \rightarrow \frac{21}{2}^{(-)}$		$\delta = -0.25 \pm 0.05$
389.9	55	0.43 ± 0.07	0.01 ± 0.09	$\frac{17}{2}^{+} \rightarrow \frac{15}{2}^{+}$		$\delta = 0.47 \pm 0.05$
397.4	34 ± 5	0.12 ± 0.05	−0.08 ± 0.05	$(\frac{13}{2}^{+}) \rightarrow \frac{11}{2}^{+}$		$\delta = 0.24 \pm 0.05$
418.5	163	0.27 ± 0.04	−0.06 ± 0.04	$\frac{19}{2}^{(-)} \rightarrow \frac{15}{2}^{(-)}$		$\delta = -0.08 \pm 0.05$
425.6	23 ± 3	−0.12 ± 0.07	−0.04 ± 0.09	$\frac{19}{2}^{+} \rightarrow \frac{17}{2}^{+}$		$\delta = 0.07 \pm 0.08$
441.5 ± 1.0	43	−0.10 ± 0.06	0.06 ± 0.08	$\frac{15}{2}^{+} \rightarrow \frac{13}{2}^{+}$	65 ± 5	$\delta = 0.09 \pm 0.05$
443.0 ± 1.0	41	−0.19 ± 0.06	−0.06 ± 0.09	$\frac{9}{2}^{+} \rightarrow \frac{7}{2}^{+}$		$\delta = -0.02 \pm 0.09$
449.3	100	0.11 ± 0.04	−0.02 ± 0.05	$\frac{11}{2}^{+} \rightarrow \frac{9}{2}^{+}$		$\delta = 0.24 \pm 0.06$
504.9 ± 1.0	24 ± 4	0.05 ± 0.08	0.07 ± 0.13			
646.6	34	−0.14 ± 0.06	−0.03 ± 0.08	$\frac{9}{2}^{+} \rightarrow \frac{7}{2}^{+}$	23 ± 5	$\delta = 0.03 \pm 0.08$
756.1 ± 0.5	32 ± 4	0.20 ± 0.08	−0.05 ± 0.09	$\frac{13}{2}^{+} \rightarrow \frac{9}{2}^{+}$	40 ± 5	$\delta = -0.13 \pm 0.13$
748.2 ± 0.6	11 ± 3			$\frac{15}{2}^{+} \rightarrow \frac{11}{2}^{+}$	17 ± 4	
814.8	157	−0.29 ± 0.10	0.07 ± 0.08	$\frac{7}{2}^{+} \rightarrow \frac{5}{2}^{+}$		$\delta = -0.22 \pm 0.12$
1047.2 ± 0.5	38	−0.56 ± 0.10	−0.13 ± 0.15			
1257.1 ± 1.0				$\frac{9}{2}^{+} \rightarrow \frac{5}{2}^{+}$		
1278.9 ± 0.6	165	0.31 ± 0.06	−0.02 ± 0.05	$\frac{15}{2}^{(-)} \rightarrow \frac{11}{2}^{-}$		$\delta = -0.02 \pm 0.06$
1347.9 ± 0.7	35	0.58 ± 0.16	−0.10 ± 0.30	$\frac{11}{2}^{-} \rightarrow \frac{5}{2}^{+}$	19 ± 6	
1460.8 ± 0.5	117	0.21 ± 0.06	−0.10 ± 0.08	$\frac{9}{2}^{+} \rightarrow \frac{5}{2}^{+}$	77 ± 5	$\delta = -0.05 \pm 0.15$

[a] Energies of γ rays are accurate to ±0.3 keV unless noted otherwise.

[b] I_γ are the γ-ray intensities, normalized such that the intensity of the $\frac{11}{2}^{+} \rightarrow \frac{9}{2}^{+}$ transition is 100; the intensities are accurate to ±10% except where noted.

[c] B.R. are the branching ratios of transitions from a given initial state.

[d] This column gives the mixing ratios $\delta(E2/M1)$, and the widths σ which describe the m-substrate population produced in the reaction (see Sec. II C).

lowed by (d,p) and (d,n). The cross sections for production of the even Sn nuclei were increasing rapidly with energy at 34 MeV, whereas those for $(^6\text{Li}, 3n)$ were nearly constant. For this reason the excitation studies could be used to help differentiate between the residual products of the two major reaction channels.

The high-spin level structures and γ-ray decay schemes of ^{113,115,117,119}Sb based on the measurements of the present study are shown in Figs. 4–7. They were deduced largely from the γ-γ coincidence results and the angular distribution information shown in Table I. The spin assignments (multipolarity information) given in Figs. 4–7 and in Table I are discussed in Sec. II B. (The assignments in brackets are less certain because the γ-ray transitions from which they were deduced did not clearly show the discussed properties for reasons of photopeak contaminants, alignment loss due to isomer feeding, or possibly non-stretched decay.) Several types of states were found to be common to all of these Sb nuclei; these systematic states will be discussed together in Sec. III A. Following this, the remaining high-spin states including lifetime and g-factor results specific to each Sb nucleus will be considered separately.

A. Level structure common to ^{113,115,117,119}Sb

The level structures observed in the four odd-mass Sb nuclei via the $(^6\text{Li}, 3n\gamma)$ reaction have several features in common at low excitation energies. These common levels have excitation energies that vary in a systematic manner as a function of A. All of the ground states were previously known to have $J^\pi = \frac{5}{2}^+$.[6,12] The first excited states, which have $J^\pi = \frac{7}{2}^+$, drop from 814 keV in ^{113}Sb to 270 keV in ^{119}Sb. An $\frac{11}{2}^-$ state exists in each case just above 1300 keV. These three levels are expected to be predominantly the proton single-particle states from the $\pi d_{5/2}$, $\pi g_{7/2}$, and $\pi h_{11/2}$ orbitals.[12,13] An unexpected and striking feature for these odd-mass nuclei is a $\Delta J = 1$ band of levels that are connected by $J \rightarrow J-1$ γ-ray cascades; the bandhead is a $\frac{9}{2}^+$ state in each nucleus. The energy spacings between corresponding states

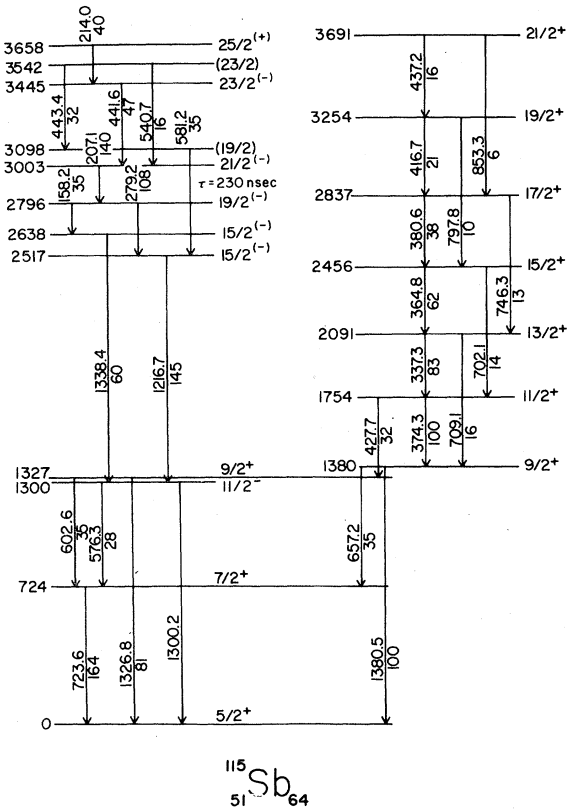

FIG. 6. The level structure and decay scheme of ^{115}Sb determined in the present study.

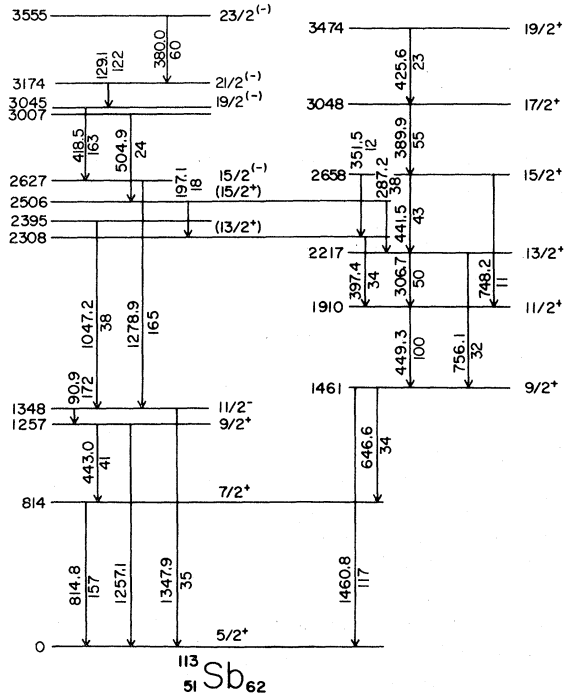

FIG. 7. The level structure and decay scheme of ^{113}Sb determined in the present study.

in these $\Delta J = 1$ bands are nearly identical for ^{115,117,119}Sb with those in ^{113}Sb showing slight increases. In addition, another $\frac{9}{2}^+$ state was observed between 1200 and 1300 keV in each odd-mass nucleus. Their excitation energies are similar to the first 2^+ state energies in the $^{A-1}$Sn cores; thus they are expected to be largely $^{A-1}\mathrm{Sn}(2^+) \otimes \pi d_{5/2}$.

As seen in the level diagrams, the first excited state in each Sb nucleus has been assigned $J^\pi = \frac{7}{2}^+$. These states decay to the ground states by γ rays whose angular distributions are characteristic of mixed dipole-quadrupole transitions. This plus additional lifetime information implies $M1/E2$ transitions and the $\frac{7}{2}^+$ assignments. These $\frac{7}{2}^+$ assignments are in agreement with those made by a (^{3}He, d) study[2] where these first excited states were populated by proton transfers of orbital angular momentum $L = 4$, indicating that they are partially composed of an odd proton in the $1g_{7/2}$ shell model orbital. The $\frac{7}{2}^+$ assignment was also made in ^{119}Sb by a ^{119}Sn(p,n) study[5] and is in agreement with β-decay studies of ^{119}Sb,[8,9] and ^{113,115}Sb.[10,11]

The spin-parity assignments for the $\frac{9}{2}^+$ bandhead and the other $\frac{9}{2}^+$ state observed between 1200 and 1300 keV in each odd-A Sb nucleus are strongly established by the γ-ray measurements. All of these states decay to the $\frac{5}{2}^+$ ground states by γ rays that have angular distributions typical of pure quadrupole transitions, which indicates a spin of $\frac{9}{2}$. Of these eight states, five decay to the $\frac{7}{2}^+$ state by γ rays whose angular distributions indicate $M1/E2$ transitions, implying $\frac{9}{2}^+$ assignments. A positive parity is also favored for these states because in all cases the quadrupole transition to the ground state competes strongly with, or dominates over, the transition to the $\frac{7}{2}^+$ state. The $\frac{9}{2}^+$ assignments are in agreement with those reported for ^{119}Sb from a β-decay study[9] and for ^{115,117}Sb from γ-ray and conversion electron measurements following (α, $2n$) reactions.[17,18]

A cascade of γ rays decaying between members of a bandlike structure was observed in each Sb nucleus to feed into the $\frac{9}{2}^+$ bandhead states discussed above. The angular distributions of the γ rays decaying between successive band members have small anisotropies, which are consistent with mixed $M1/E2$ $J \to J-1$ transitions (positive mixing ratios). This is corroborated by the occurrence of weaker crossover γ rays that have properties characteristic of $E2$ $J \to J-2$ transitions. Lifetime limits for these states rule out the importance of higher multipolarities. On the basis of these arguments, the states in the bands were assigned $J^\pi = \frac{9}{2}^+, \frac{11}{2}^+, \frac{13}{2}^+, \ldots$; seven members with J^π up to $\frac{21}{2}^+$ were identified in the ^{115}Sb band. The spin

assignments for band members in ^{115,117}Sb are in agreement with those based on $(\alpha, 2n)$ conversion-electron studies.[17,18]

The $J^\pi = \frac{11}{2}^-$ states identified at energies just above 1300 keV in the odd-mass Sb nuclei are firmly established by the present γ-ray measurements. The angular distribution data indicate that these states decay in one or more of the following branches: a dipole transition to one of the $\frac{9}{2}^+$ states discussed, a quadrupole transition to the $\frac{7}{2}^+$ first excited state, and/or an octupole transition to the $\frac{5}{2}^+$ ground state. These angular distributions strongly imply the $J^\pi = \frac{11}{2}^-$ assignments. The observed branching is also consistent with the multipolarities and energies of the transitions. The $\frac{11}{2}^-$ assignments for these states in ^{113,117,119}Sb are in agreement with the (^{3}He, d) studies,[2] where these states were populated by proton transfer of orbital angular momentum $L = 5$ that indicates the presence of $1h_{11/2}$ proton strength. The assignment was also suggested by β-decay studies in ^{119}Sb[9] and conversion electron measurements[17,18] in ^{115,117}Sb.

B. States in ^{119}Sb

In addition to the previously discussed results for ^{119}Sb a 948-, 237-, and 288-keV γ-ray cascade was found in coincidence with the decay γ rays of the $\frac{11}{2}^-$ state at 1365 keV. From the relative intensities of the γ rays, excited states were identified at 2314, 2552, and 2840 keV as shown in Fig. 4. This identification is strengthened by the observation of the 135-keV γ ray that branches from the 2552-keV level to the 2419-keV $\frac{17}{2}^+$ band member. The states at 2314, 2552, and 2840 keV were assigned spins of $\frac{15}{2}^{(-)}$, $\frac{19}{2}^{(-)}$, and $(\frac{21}{2}^-)$, respectively, on the basis of the γ-ray information given in Table I. Unfortunately, these states were fed significantly from a long-lived isomer, which attenuated the anisotropy of their decay γ rays and thus made it difficult to extract precision angular distribution information.

The mean lifetime of the isomeric state was measured to be $\tau = 1.23 \pm 0.13$ sec with the ^{6}Li beam pulsed at a 3 s repetition period. Data for this measurement are presented in Fig. 8 which displays energy spectra collected for different delayed time regions. All of the states observed in the present study of ^{119}Sb were found to be partially populated via the long-lived isomer. A time spectrum collected for the 288-keV γ ray showed, after the Compton background was subtracted, that $(12 \pm 2)\%$ of this transition is prompt. This indicates that the 2840-keV level is not the isomer, but that the isomer decays by an unobserved transition to this level. A tentative spin assignment

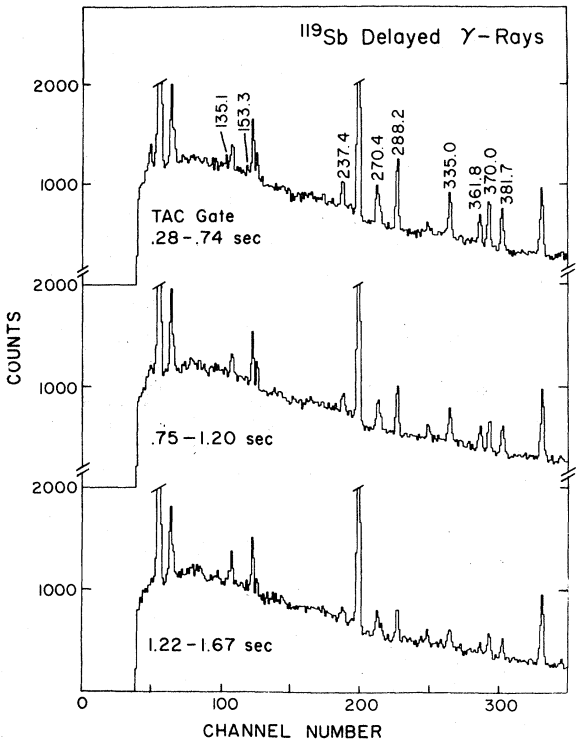

FIG. 8. Delayed γ-ray spectra for several delayed time regions obtained from the ^{116}Cd(^{6}Li, $3n$)^{119}Sb reaction with the beam pulsed at a 3 s repetition period.

$J^\pi = (\frac{27}{2}^+)$ has been made for the isomer on the basis of its lifetime, which is approximately consistent with Weisskopf estimates for a 50-keV $E3$ or 200-keV $M3$ transition depopulating the isomer. A 50-keV $E3$ is preferred because it would have an interval conversion coefficient $\alpha > 200$, whereas a 200-keV $M3$ transition would have $\alpha \sim 2$ and should have been observed in the delayed spectra. A quadrupole transition corresponding to $J = \frac{25}{2}$ for the isomer is unlikely because exceptionally large hindrances would be required. The ^{119}Sb decay scheme and this isomer have also been studied recently using $(p, xn\gamma)$ reactions.[7]

C. States in ^{117}Sb

In ^{117}Sb a group of states was located by the γ-ray measurements between 2300 and 3200 keV; their excitation energies are 2323, 2525, 2779, 2874, 3072, and 3130 keV as shown in Fig. 5. The spin assignments shown for these states are based on the present angular distribution and lifetime information. The position of a weak 568-keV γ ray could not be firmly established in the decay scheme. All γ rays except the 433-keV and 568-keV γ rays were observed to be fed by the previously known[17] isomeric state ($\tau = 340$ μsec) at 3130 keV. Partial feeding from this isomer re-

sulted in attenuation of some of the γ-ray angular distributions.

Many of the high-spin states have previously been investigated by γ-ray measurements following the ^{115}In$(\alpha, 2n)$ reaction.[17] This earlier study observed all of the levels known in Fig. 5 except the 3057- and 3625-keV levels. Spin-parity assignments, based on measurements of conversion electrons, were made in this previous study. These previous assignments are in agreement with those given in the present study. The $(\alpha, 2n)$ work observed $\tau = 340$ μs isomer and assigned it to be 3130-keV level, in agreement with the present pulsed beam results. Recently, a $(p, xn\gamma)$ study[7] of ^{117}Sb obtained results in agreement with those given here for states up to the 2323-keV level.

D. States in ^{115}Sb

A group of eight states was observed in ^{115}Sb between 2500 and 3700 keV by the various γ-ray measurements as shown in Fig. 6. The γ-ray decay of these states feed into the $\frac{11}{2}^+$ state at 1300 keV that was discussed previously.

In pulsed beam studies, several ^{115}Sb γ rays were observed to have delayed components showing the same lifetime slope. These γ rays included two pairs of coincident γ rays, (279-1217) and (158-1338) keV, which feed the 1300-keV $\frac{11}{2}^-$ state. Several measurements of the delayed components gave a mean lifetime value $\tau = 230 \pm 4$ ns. Typical data for this pulsed beam-γ measurement are presented in Fig. 9 which shows a time spectrum for the Compton-subtracted photopeak of the 279-keV γ ray. The coincidence data and γ-ray energy sums imply a level at 2796 keV that decays via these γ-ray cascades to the $\frac{11}{2}^-$ state. The γ rays were ordered within the cascades as shown in Fig. 6 on the basis of their intensities. From the γ-ray angular distributions, the resulting states at 2517 and 2638 keV were assigned $J = \frac{15}{2}^{(-)}$. The fact that there is no prompt peak in the time spectrum for the 279-keV γ ray shown in Fig. 9 implies that the 2796-keV level is the isomer. The $\tau = 230$ ns mean lifetime of this level is roughly consistent with Weisskopf estimates for its decay by quadrupole transitions, but is a factor of $>10^5$ slower than such estimates for dipole transitions. The 279-keV decay γ ray could either be a normal $M2$ or a hindered $E2$ transition relative to Weisskopf estimates, while the 158-keV transition could be a normal $E2$ or an enhanced $M2$. The angular distributions of these two γ rays are strongly attenuated because of the isomeric lifetime. On the basis of this lifetime information, the 2796-keV isomer is assigned $J = \frac{19}{2}^{(-)}$.

The g factor of the 2796-keV level was measured by the TDPAD method with an external magnetic

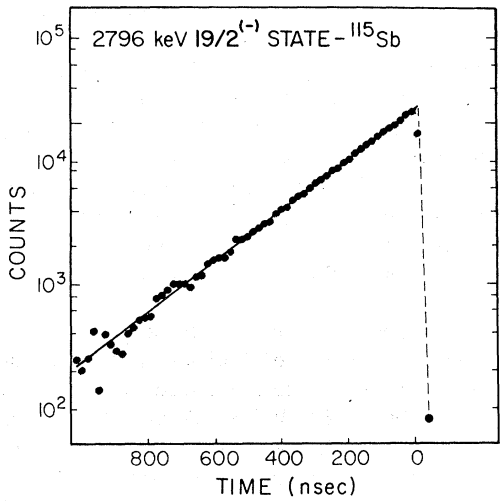

FIG. 9. A Compton-subtracted time spectrum collected for the 279-keV γ ray in ^{115}Sb with the beam pulsed at a repetition period of 1 μs. The solid line is a least-squares fit to an exponential decay.

field, as discussed in Sec. II E. Typical ratio spectra $R(t)$ collected are shown in Fig. 10. An uncorrected value $|g| = 0.290 \pm 0.005$ was extracted from several runs.[20] Expected corrections to the external magnetic field are given by the relation $B = B_{\text{ext}}(1+\sigma)(1+K)$, where σ is the diamagnetic shielding correction and K is the Knight shift. Although neither σ nor K has been measured for Sb in Cd, good estimates can be made. A value $\sigma = -0.006 \pm 0.001$ is expected in the $Z = 53$ region on the basis of electron shielding calculations including relativistic effects.[39] A Knight-shift calculation based on related measurements yields $K \simeq +0.007$.[40] Since σ and K are small and nearly cancel each other, the corrected g factor is equal to the uncorrected value with the uncertainties unchanged. The preliminary reports[20,38] of this measurement gave the sign of the g factor as negative. Recently, independent measurements of this

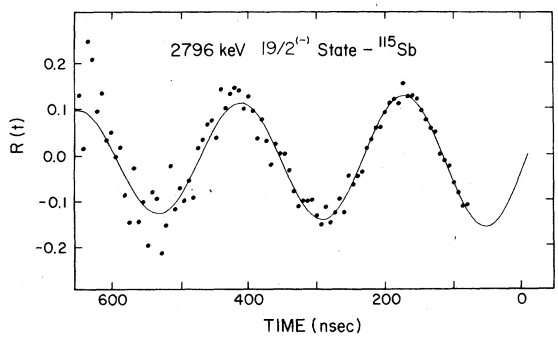

FIG. 10. The ratio spectrum $R(t) = [Y(-135°, t) - Y(135°, t)]/[Y(-135°, t) - Y(135°, t)]$ collected in the TDPAD g-factor measurement for the $\tau = 230$ ns isomer at 2796 keV in ^{115}Sb.

g factor have been made via α induced reactions on In targets; preliminary results from these measurements indicated agreement of the absolute value of the g factor but gave a positive sign.[41,42] A reanalysis of the initial g-factor measurement[20] and the subsequent radiation-damage study of Sb recoils in Cd as a function of temperature[38] also yielded a positive sign, namely $g = +0.290 \pm 0.005$. A misinterpretation of the phase in the ^{69}Ge ratio data, that was used for the magnetic field calibration, had caused the reversed sign.

Five states were identified above the 2796-keV level, up to an energy of 3658 keV and a spin of $\frac{25}{2}$. The 2796-keV state was found to be fed by a strong 207-442-214 keV cascade of γ rays. The bottom two γ rays had anisotropies that strongly indicate mixed dipole-quadrupole transitions, while the 214-keV γ ray was consistent with a pure dipole. Thus, states at 3003, 3445, and 3658 keV were assigned spins of $\frac{21}{2}^{(-)}$, $\frac{23}{2}^{(-)}$, and $\frac{25}{2}^{(+)}$, respectively. Also states at 3098 keV and 3542 keV were located by a weak 581-443 keV γ-ray coincidence and assigned spins of $(\frac{19}{2})$ and $(\frac{23}{2})$, respectively.

Recently high-spin states in ^{115}Sb have also been investigated via the $(\alpha, 2n\gamma)$ reaction.[18] The results of this study agree with those of the present work, except for a difference in the ordering of the 443-keV and 582-keV coincident γ rays. However, these γ rays are weak and the intensities quoted in both studies are consistent with either ordering. The $(\alpha, 2n\gamma)$ study included conversion electron measurements from which additional parity information was extracted. They assigned negative parity to the eight states above 2500 keV shown in Fig. 6 that feed into the 1300 keV $\frac{11}{2}^-$ state, except for the 3658-keV $\frac{25}{2}$ state to which they assigned positive parity. They also obtained a lifetime result for the 2796-keV isomer in agreement with the present work as well as mean lifetimes of $\tau = 5.8 \pm 0.3$ and 9.7 ± 0.6 ns, respectively, for the 3658- and 1300-keV states. Several high-spin states in ^{115}Sb have also been observed with the $(p, 2n\gamma)$ reaction[19]; results consistent with those of the present work were obtained for the $\Delta J = 1$ band members with $J \leq \frac{17}{2}$.

E. States in ^{113}Sb

In ^{113}Sb, an additional group of states above 2300 keV was observed by the γ-ray measurements as shown in Fig. 7. A strong 1279-418-129-380 keV γ-ray cascade fed the $\frac{11}{2}^-$ state at 1348 keV. The bottom two γ rays in the cascade had quadrupole properties and the upper two showed a mixed dipole-quadrupole character. On this basis, levels at 2627, 3045, 3174, and 3555 keV were assigned spins of $\frac{15}{2}$, $\frac{19}{2}$, $\frac{21}{2}$, and $\frac{23}{2}$, respectively, and (−) parities.

As shown in Fig. 7, there are several other weaker γ rays which document additional levels in ^{113}Sb. In particular, levels at 2308 and 2506 keV which have been tentatively assigned $(\frac{13}{2}^+)$ and $(\frac{15}{2}^+)$ are connected by γ rays with the $\Delta J = 1$ band members that are displayed on the right side of Fig. 7.

High-spin states in ^{113}Sb have also been studied with the $(p, 2n\gamma)$ reaction[19] which yielded information on several states with $J \leq \frac{13}{2}$. These results are in agreement with the present work.

IV. DISCUSSION

The low-lying level spectra in odd-mass Sb nuclei are expected to include spherical single-particle states since the Sb nuclei ($Z = 51$) have one proton beyond the major shell closure at $Z = 50$. These states will be discussed in Sec. IV A. In addition to the single-particle states, two-particle one-hole (2p-1h) states can be formed by the excitation of a proton out of a lower shell. In each of these Sb nuclei, a $\frac{9}{2}^+$ state has been identified and interpreted as a deformed 2p-1h state involving the excitation of a $1g_{9/2}$ proton across the $Z = 50$ closed shell. The energies of these states which are also shown in Fig. 11, decrease rapidly from 1461 keV to 971 keV in going from ^{113}Sb to ^{119}Sb. These intruder states will be discussed further in Sec. IV B.

Other states in the odd-mass Sb nuclei are expected to involve the coupling of an odd-proton, in any of the single-particle orbitals, to excitations of the core. Since the cores of the odd-mass ^{A}Sb nuclei are the $^{A-1}$Sn nuclei, these states are expected for weak coupling to be roughly equal

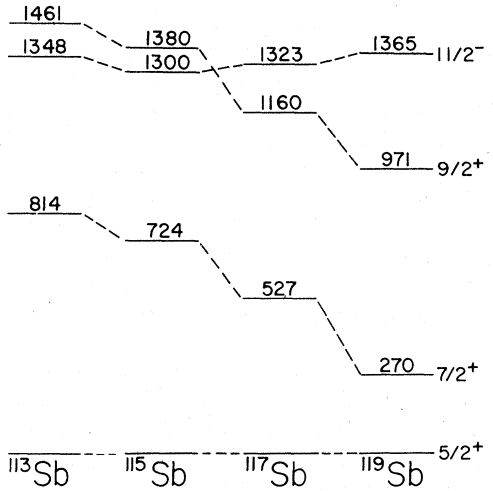

FIG. 11. A diagram of the excitation energies of low-lying high-spin states in odd-mass Sb nuclei.

to the excited states of the neighboring even Sn nuclei. The excitations in the Sn cores are usually described as phonon vibrations or as two-neutron quasi-particle states formed by the breaking of a neutron pair. The states in Sb that are interpreted as an odd proton coupled to these core excitations will be discussed in Sec. IV C.

A. Single-particle states

The high-spin single-particle states at low energy in the odd-mass Sb nuclei are expected to have the valence proton occupying the $2d_{5/2}$, $1g_{7/2}$, or $1h_{11/2}$ shell model orbitals. In the ^{113,115,117,119}Sb nuclei, states of $J^\pi = \frac{5}{2}^+$, $\frac{7}{2}^+$, and $\frac{11}{2}^-$ were observed which have previously been interpreted[12,13] as these single-particle states. The energies of these states are summarized in Fig. 11. As can be seen in this figure, the $\frac{11}{2}^-$ states have a relatively constant energy with respect to the $\frac{5}{2}^+$ ground states, whereas the $\frac{7}{2}^+$ states decrease sharply in energy as a neutron number increases. The spectroscopic factors from (^{3}He, d) studies[2] indicate that the $\frac{5}{2}^+$ and $\frac{7}{2}^+$ states contain most (80–90%) of the $2d_{5/2}$ and $1g_{7/2}$ single-particle strengths in all four of the odd-mass Sb nuclei. The $\frac{11}{2}^-$ states, except for that in ^{115}Sb which was not observed with this reaction, were found to have smaller single-particle strengths (~50%).

B. Deformed $\frac{9}{2}^+$ intruder states and the $\Delta J = 1$ bands

In each Sb nucleus, a $\frac{9}{2}^+$ state was observed to be fed by a bandlike cascade of $J \to J-1$ γ-ray transitions with $J \to J-2$ crossovers. These cascades and $\Delta J = 1$ bands are shown on the right side of Figs. 4–7. As shown, very few γ-ray transitions into or out of the bands occur. The similarity of the energies of the γ rays in these cascades is most striking as can be seen in Fig. 12, which shows the $\Delta J = 1$ band members plotted relative to the energy of the $\frac{9}{2}^+$ bandhead. Very recently the $\Delta J = 1$ bands built on $\frac{9}{2}^+$ proton hole states in ^{121,123}Sb have been observed via γ-ray measurements following the ^{120,122}Sn(^{6}Li, $\alpha 2n$) reactions.[21] The $\Delta J = 1$ energy spacings observed from the bottom are 375, 328, 349, and 359 keV in ^{121}Sb; and preliminary 438 and 370 keV in ^{123}Sb. These $\Delta J = 1$ bands are included in Fig. 12.

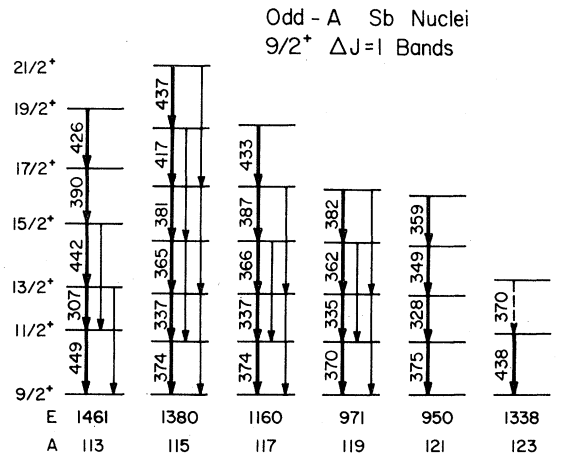

FIG. 12. A level diagram of the $\Delta J = 1$ bands in ^{113,115,117,119,121,123}Sb plotted relative to the $\frac{9}{2}^+$ bandheads.

The observed similarities suggest a common structure of these $\Delta J = 1$ bands in the odd-mass Sb nuclei. In particular, a rotational interpretation[27–30,15] for these bands is implied by the following properties: (1) the energy spacings between band members, (2) the mixing ratios $\delta(E2/M1)$ of the $J \to J-1$ transitions, (3) the relative intensities of the $J \to J-1$ and $J \to J-2$ crossover transitions, and (4) the $\frac{9}{2}^+$ bandhead energies as a function of neutron number N. This rotational interpretation will be developed in this section. Part of the $\frac{9}{2}^+$ band in ^{117}Sb shown in Fig. 6 was previously observed via the ^{115}In($\alpha, 2n$)^{117}Sb reaction by Fromm *et al.*[17] They interpreted their γ-ray and conversion electron data for the $\Delta J = 1$ cascade in terms of a rotational band of a symmetric prolate rotor.

The $\Delta J = 1$ bands of the odd-mass Sb nuclei shown in Fig. 12 might also be interpreted in terms of a quasiparticle or cluster coupled to anharmonic phonons of the core. It has been shown that such models can describe $\Delta J = 1$ bands in transitional nuclei.[31–33,16] A vibrational model has been applied to the $\Delta J = 1$ band in ^{115}Sb by Bron *et al.*[18] as observed in their ($\alpha, 2n$) experiment. Our preference for a rotational interpretation is based on the fact that the low-lying $\frac{9}{2}^+$ bandheads are difficult to understand in the vibrational models.

1. Rotational interpretation of the $\Delta J = 1$ bands

The energy spacings in the bands are roughly in agreement with the spacings expected for a rotational band. A simple check on the consistency of the band spacings and a rotor moment of inertia can be made using the approximate formula for energies of an axially symmetric rigid rotor, $E_J = (\hbar^2/2\mathcal{I})J(J+1)$, where E_J is the energy of a band member of spin J and $\mathcal{I}$ is the moment of inertia. Although deviations from this equation are expected from the Coriolis interaction or from possible axial asymmetries of the core, the simple formula should give a reasonable estimate of the moment of inertia. Values of $(2\mathcal{I}/\hbar^2) = 2J/(E_J - E_{J-1})$ are plotted for $J \to J-1$ transitions in ^{115}Sb in Fig. 13. As shown, $(2\mathcal{I}/\hbar^2)$ varies from ~ 29 MeV^{-1} at the bottom of the band ~ 48 MeV^{-1} at the top. Results for ^{117,119,121}Sb are

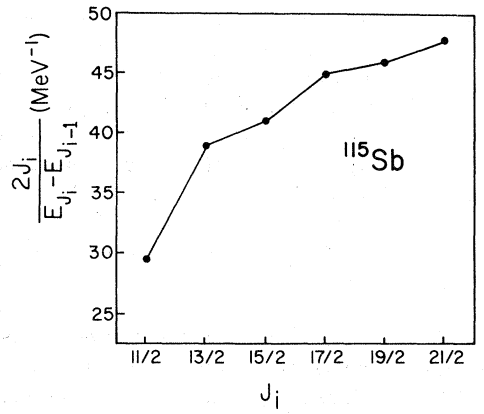

FIG. 13. A plot of the moment of interia $(2\mathcal{I}/\hbar^2)=2J/(E_J-E_{J-1})$ against $J=J_i$ for the $\Delta J=1$ band in ^{115}Sb.

nearly identical to those for ^{115}Sb, while those for ^{113,123}Sb are 5–10% smaller. As will be discussed later, calculations using a more sophisticated model that takes into account the Coriolis interaction and possible core asymmetries can reproduce the observed energy levels reasonably well with a unique moment of inertia for each nucleus.

Evidence for a rotational interpretation of the Sb bands is also obtained from the experimental mixing ratios $\delta(E2/M1)$ of the $J\rightarrow J-1$ transitions within the bands. When mixing ratios are calculated using transition probability expressions for an axially symmetric rotor,[27] a reasonable agreement with the experimental values is obtained for an intrinsic quadrupole moment $Q_0=+3.0$ barns. This quadrupole moment corresponds to a deformation $\beta\sim 0.2$ for an axially symmetric, uniformly charged nucleus. Because the experimental mixing ratios have rather large uncertainties, they do not provide a sensitive measure of Q_0. Nevertheless, the angular distributions for each case clearly define $\delta(E2/M1)>0$ for the $J\rightarrow J-1$ transitions, so that Q_0 must be positive,[43] and the deformation prolate, in this model. The moment of inertia $\mathcal{I}$ extracted from rotational band spacings usually lies between $\frac{1}{2}$ and $\frac{1}{3}$ of the rigid-rotor $\mathcal{I}$ defined for a deformation β[44]; since the extracted moments of inertia $\mathcal{I}$ in the odd-mass Sb nuclei lie within this range for $\beta\sim 0.2$, the band spacings are consistent with this deformation.

The experimental ratios of the intensity of a $J\rightarrow J-1$ transition to the intensity of the $J\rightarrow J-2$ crossover $E2$ transition give an additional test for the rotational interpretation of the Sb bands. The $E2$ crossover transitions are enhanced such that these experimental intensity ratios within uncertainties are consistent with values calculated for an axially symmetric rotor[27] with $Q_0=3.0$ barns. Thus the band spacings, mixing ratios $\delta(E2/M1)$, and ratios of intensities of the $J\rightarrow J-1$ and $J\rightarrow J-2$ crossover transitions together all point to the interpretation of the bands in ^{113,115,117,119}Sb as rotational bands. As will be discussed later, more detailed calculations of the band spacings and the electromagnetic properties in a deformed rotor model, which compare favorably with the experimental results, strengthen this interpretation.

The deformation of the $\frac{9}{2}^+$ bandheads implied by the experimental results are reasonable in view of the Nilsson orbitals available at prolate deformations in this nuclear region. Calculated energies of Nilsson orbitals as a function of deformation for ^{115}Sb are shown in Fig. 14; these are taken from a recent article by Heyde *et al.*[15] As Fig. 14 shows, the $[404]\frac{9}{2}^+$ orbital rises sharply at positive deformations. Therefore, the state formed by exciting a proton out of the $[404]\frac{9}{2}^+$ orbital can decrease in energy as the deformation increases provided the core is soft to deformation; a significant decrease in energy is expected at a deformation $\beta\sim 0.2$ ($\epsilon\sim 0.12$). These energy arguments suggest that the $\frac{9}{2}^+$ states in ^{113,115,117,119}Sb are deformed 2p-1h states with the proton hole in the $[404]\frac{9}{2}^+$ orbital. The decrease in energy of the proton-hole orbital at positive deformation results in a binding energy gain if the potential energy of the core does not rise too quickly at these deformations. Such a gain in binding energy is required if the $\frac{9}{2}^+$ bandheads are $[404]\frac{9}{2}^+$ proton-hole states because these states are expected to have energies of $\gtrsim 2.5$ MeV in a nearly spherical nucleus.[15,45]

Further evidence for the 2p-1h interpretation is

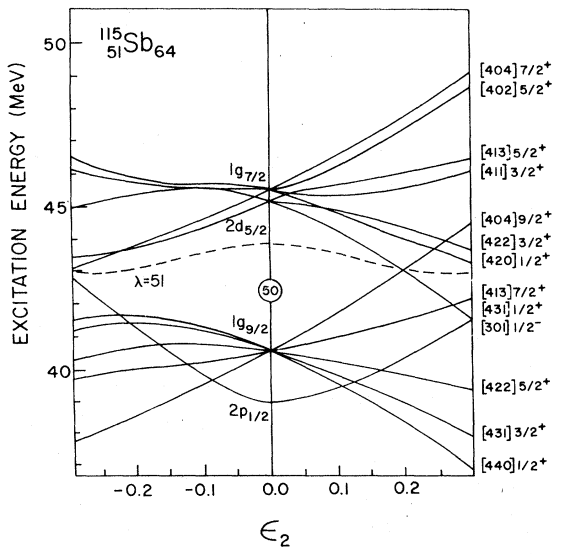

FIG. 14. A diagram of the single-particle energy levels for ^{115}Sb as a function of the axially symmetric core deformation ϵ_2, calculated by Heyde *et al.* (Ref. 15).

obtained from the energy systematics of $\frac{9}{2}^+$ proton-hole states observed with $L=4$ pickup strength in the odd-mass $^{121-129}$Sb nuclei by the (t,α) reaction[4] and in ^{119}Sb by the (p,α) reaction.[46] The energies of these proton-hole states increase from a minimum of 950 keV in ^{121}Sb to 2710 keV in ^{129}Sb; they are plotted as a function of neutron number N in Fig. 15 together with the energies of the $\frac{9}{2}^+$ bandheads observed in $^{113-119}$Sb in the present work and in the ^{121,123}Sb nuclei.[21] These energy systematics show that the energies of the deformed $\frac{9}{2}^+$ bandheads are equal to or continuous with those of the $\frac{9}{2}^+$ proton-hole states identified in the pickup-reaction studies.

The minimum in these $\frac{9}{2}^+$ excitation energies near ^{119,121}Sb as shown by the dashed curve in Fig. 15 suggests a deformation maximum near the middle of the neutron shell, while the increased energies of the $\frac{9}{2}^+$ proton-hole states in the heavier and lighter odd-mass Sb nuclei suggest that the deformation decreases as N approaches the closed shells at $N=82$ and 50. The decrease in the excitation energy of the $\frac{9}{2}^+$ proton-hole orbital resulting from an increased deformation is expected to be roughly proportional to β where the proportionality constant is related to the slope of the $[404]\frac{9}{2}^+$ Nilsson orbital. The moments of inertia $\mathcal{I}$ extracted from the band spacings yield direct information on the deformation in that β is approximately proportional to $\sqrt{\mathcal{I}}$. The value of $(2\mathcal{I}/\hbar^2)^{1/2}$ for the odd-mass Sb nuclei extracted from the energy difference between $\frac{13}{2}^+$ and $\frac{9}{2}^+$ band members (this choice avoids possible shifts in the $\frac{11}{2}^+$ member due to deformation asymmetries) are plotted in Fig. 16 on an inverted scale as a function of N. The dashed curve drawn through the excitation energies in Fig. 15, which is roughly parabolic with a narrow minimum at $N=68$–70, does not have

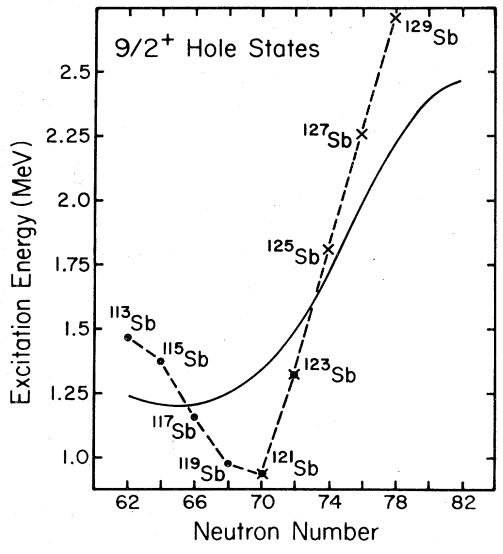

FIG. 15. The energy systematics for the $\frac{9}{2}^+$ hole states in the odd-mass $^{113-129}$Sb nuclei. The circles are from the present study and Ref. 21; the crosses are from (t,α) pickup reaction studies (Ref. 4). For comparison, energies of the $[404]\frac{9}{2}^+$ hole states calculated by Heyde, *et al.* (Ref. 15) are plotted as a solid line.

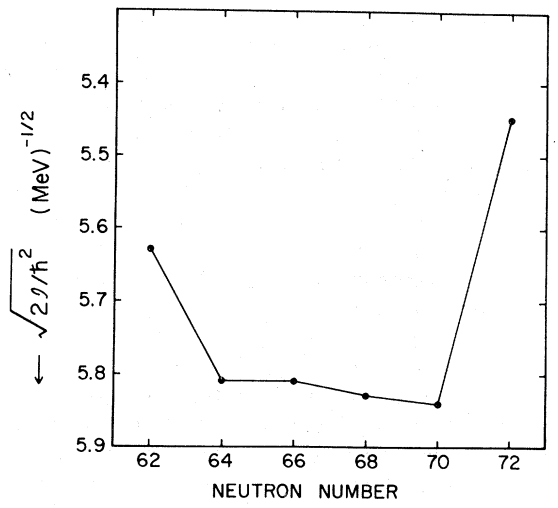

FIG. 16. The quantity $(2\mathcal{I}/\hbar^2)^{1/2}$ extracted from the $\Delta J=1$ band spacings in the odd-mass Sb nuclei plotted against the neutron number N. This quantity is approximately proportional to the deformation. The data points for $N=70,72$ are taken from Ref. 21.

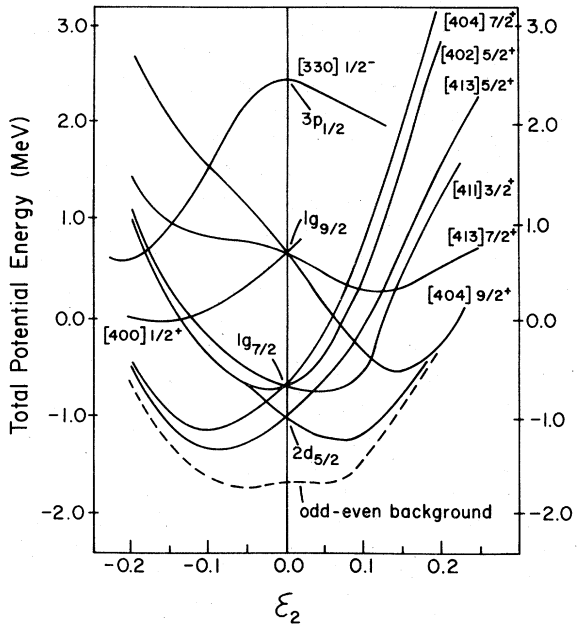

FIG. 17. Calculated energies of various states in ^{115}Sb as a function of deformation ϵ_2. Taken from Heyde *et al.* (Ref. 15). The dashed curve is the potential energy of the even core for ^{115}Sb as deduced from the neighboring nuclei.

the identical shape as the curve in Fig. 16 drawn through the values of $(2\mathcal{I}/\hbar^2)^{1/2}$ for $^{113-121}$Sb. In particular, the maximum in the moment of inertia curve appears broader than the minimum in the excitation energies and possibly shifted down to $N \approx 66$. This difference in shapes as a function of N implies that, in addition to the deformation, the neutron-proton and pairing interactions are also varying as a function of N so as to influence the excitation energies of these $\frac{9}{2}^+$ proton-hole states. These interactions are in themselves very interesting for the $Z > 50$ transition region.

A theoretical study of the $[404]\frac{9}{2}^+$ proton-hole states in the odd-mass $^{113-133}$Sb nuclei has recently been performed by Heyde *et al.*[15] The total energies including the potential energy of the core were calculated as a function of an axially symmetric deformation parameter ϵ. An example of these calculations is given in Fig. 17 for various states of ^{115}Sb. As shown, the state consisting of a proton hole in the $[404]\frac{9}{2}^+$ orbital decreases rapidly in energy as the deformation increases reaching a minimum energy at $\epsilon \sim 0.15$; the extracted excitation energy at the minimum deformation is ~1.2 MeV, in reasonable agreement with the experimental value. The excitation energy for the $[404]\frac{9}{2}^+$ proton-hole states for all of the odd-mass Sb nuclei calculated by Heyde *et al.*[15] are shown in Fig. 15 by a solid line along with the experimental energies. Figure 15 demonstrates that the calculations reproduce the general dependence of the excitation energies of these $\frac{9}{2}^+$ states as a function of neutron number. The deformation extracted at the energy minima are in fair agreement with the values deduced from the experimental band properties.

Further information on deformed $\frac{9}{2}^+$ proton-hole states in this $Z > 50$ transition region has been obtained from studies of high-spin states in the odd-mass $^{117-127}$I ($Z = 53$) nuclei,[23] and $^{119-125}$Cs ($Z = 55$) nuclei.[24] In these studies, $\Delta J = 1$ bands built on low-lying $\frac{9}{2}^+$ states were observed (see Fig. 18); these bandheads are interpreted as 4p-1h and 6p-1h states in the I and Cs nuclei, respectively. The energy systematics of the deformed $\frac{9}{2}^+$ proton-hole states in Sb, I, and Cs are similar in that they follow parabolic shapes as shown in Fig. 19 with a minimum energy near the center of the neutron shell ($N = 66$); the energy minima are at $^{119-121}$Sb (~950 keV), at ^{119}I(~300 keV), and in ^{119}Cs the $\frac{9}{2}^+$ state becomes the ground state. Very recently, a $\Delta J = 1$ $\frac{9}{2}^+$ band was observed in ^{125}La.[25]

A deformed structure relationship between the excitation of a $1g_{9/2}$ proton from the $Z = 50$ closed core and the excitation of a pair of $1g_{9/2}$ protons has recently been made. Low-lying deformed 0_2^+

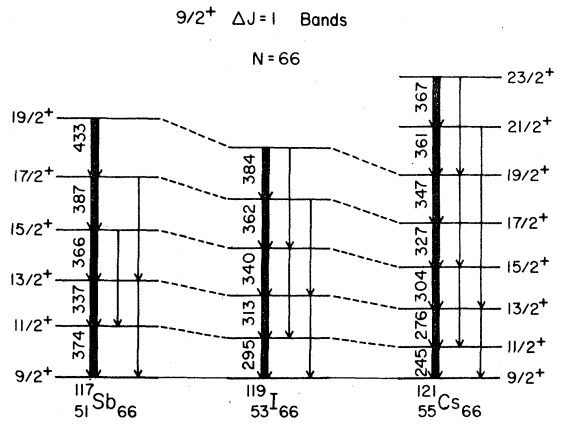

FIG. 18. A comparison of the $\frac{9}{2}^+$ $\Delta J = 1$ band for the $N = 66$ isotones of ^{117}Sb, ^{119}I (Ref. 23), and ^{121}Cs (Ref. 24).

states in even Sn ($Z = 50$) nuclei have been identified by Bron *et al.*[47] from the observation of their rotational bands via $(\alpha, 2n\gamma)$ studies. These 0_2^+ states have a large $L = 0$ Cd(^{3}He,n) strength implying a significant $(1g_{9/2})^{-2}$ proton component. The moments of inertia extracted from the band spacings of these 2p-2h 0_2^+ states in the Sn nuclei are slightly greater than those of the corresponding 2p-1h $\frac{9}{2}^+$ states in the Sb nuclei. In addition, the parabolalike curves connecting the bandhead energies for the 0_2^+ Sn and $\frac{9}{2}^+$ Sb states have similar shapes and minima as a function of N (see Fig.

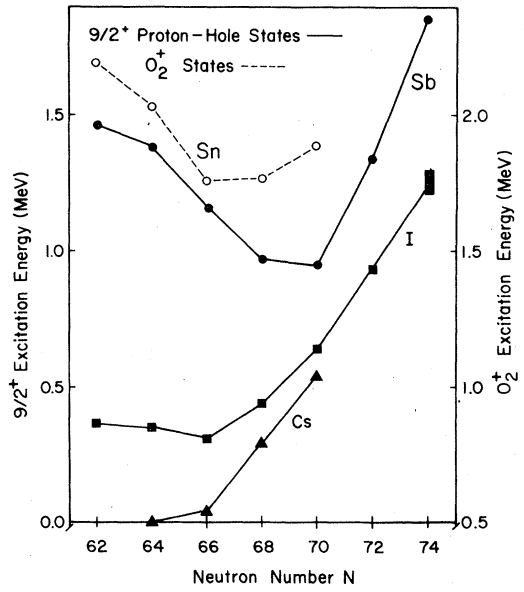

FIG. 19. The $\frac{9}{2}^+$ bandhead energies as a function of neutron number N for the Sb, I, and Cs isotopes (Refs. 21, 23, 24). For comparison, the 0_2^+ bandhead energies in the even Sn isotopes (Ref. 47) are also included.

19). These similar deformation properties suggest that the deformed $\frac{9}{2}^+$ (2p-1h) Sb states are better represented by a coupling of a proton to the 0_2^+ (2p-2h) Sn states than by a coupling of a proton hole to the (2p) Te ground states that are at most only modestly deformed.

The energies and deformations of these proton-hole states as a function of N and Z contain information sensitive to the nuclear potential energy surface for this transition region. A detailed mapping of the deformation properties of the $1g_{9/2}$ proton excitations is theoretically important for an understanding of these intruding collective features.

2. *Consideration of axially asymmetric deformations*

Although band mixing calculations in an axially symmetric model can generally describe the $\Delta J = 1$ bands observed in the odd-mass Sb nuclei, the possibility of axially asymmetric core deformations should be considered. Properties of rotational bands with axially asymmetric deformations have been studied by Davydov and Filipov,[48] and more recently by Meyer-ter-Vehn.[29] In these studies, for which the nuclear deformation is parametrized by a deformation β and by an asymmetry γ, the level spacings for odd-mass nuclei were found to be especially sensitive to γ. Thus, comparison calculations of the $\Delta J = 1$ band spacings in the Sb nuclei were made to investigate the degree of asymmetry.

In the Sb bands, the spacings reveal consistent deviations from those expected for a typical symmetric rotor with Coriolis corrections. All four of the Sb bands show a squeezing of the $\frac{13}{2} - \frac{11}{2}$ spacing ($\frac{11}{2}$ state is pushed up) relative to the other spacings. Such a $(j+2) - (j+1)$ squeezing occurs as γ increases from 0° for hole states[29] and suggests that these bands can be described by a value of $10° < \gamma < 30°$. These deviations are not likely to be caused by admixtures from other states, since the band spacings are nearly identical in $^{115-119}$Sb, while the energies of states that could admix with the band members are expected to vary significantly with respect to the energies of the band members.

To carry out the investigation of a deformation asymmetry, calculations were made for these $\Delta J = 1$ bands using the triaxial rotor model of Meyer-ter-Vehn,[29] which includes an unattenuated Coriolis interaction. In these calculations, a pairing gap of $\Delta = 1.2$ MeV was used and the Fermi level was taken to be at the highest single-particle state of the $g_{9/2}$ orbital. The best theoretical description of the ^{115}Sb band was obtained with $\gamma = 20°$ and $\beta = 0.317$. The band energies calculated with these parameters are shown on the right-hand side of Fig. 20, along with the experimental energies. As shown, the calculated energies agree with the experimental energies within a few keV for the lower levels. For the higher levels, the calculation begins to show differences which may result from the neglect of high-spin centrifugal stretching or of small core vibrations about the equilibrium deformation. For comparison, the results of a calculation with $\gamma = 0°$ (axial symmetry) are also shown in Fig. 20. Here the value of β was chosen to give the same overall energy spacings as the $\gamma = 20°$ calculation. As can be seen, the calculation with $\gamma = 0°$ does not give the observed band spacings; in particular, the squeezing of the $\frac{13}{2} - \frac{11}{2}$ levels was not reproduced. The $\Delta J = 1$ bands built on the $\frac{9}{2}^+$ proton-hole states in the odd-mass I and Cs nuclei,[23,24] however, did not show the $\frac{13}{2} - \frac{11}{2}$ squeezing and could be fit well with $\gamma = 0°$ (see Fig. 18).

Although the symmetric band-mixing calculations of Heyde *et al.*[15] and Van Isacker *et al.*[16] that also include the Coriolis interaction give reasonable fits to the $\Delta J = 1$ Sb bands, the $\frac{13}{2} - \frac{11}{2}$ squeezing was not fit as well. Since the triaxial-rotor model fits this squeezing in a natural way as a function of γ it appears in our opinion to be a more realistic model and thus a more appropriate starting point for theoretical calculations.

The failure of the triaxial rotor model of Meyer-ter-Vehn to predict the details of the high-spin band members is in part because the model as-

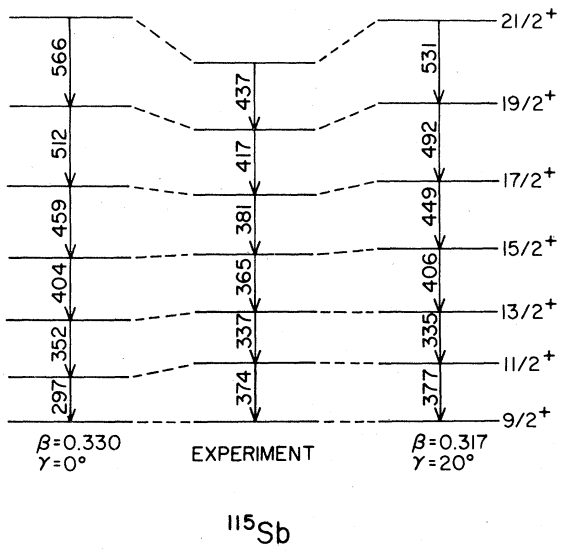

FIG. 20. A comparison of the rotational band observed in ^{115}Sb with calculations from the triaxial rotor model of Meyer-ter-Vehn (Ref. 29). Both the best fit, $(\beta, \gamma) = (0.317, 20°)$, and the axially symmetric case, $\gamma = 0°$ are shown.

sumes a rigid core with fixed values of β and γ. Time dependent variations of these deformation parameters from vibrations and centrifugal stretching are expected to have an effect. Unfortunately, the treatment of both vibrational and rotational degrees of freedom in odd-mass nuclei is a complex problem which can only be handled in a limited manner at present. A recent development in the triaxial rotor model has been made by Toki and Faessler,[30] who have included an increasing moment of inertia for the core to account for possible centrifugal stretching. This also approximately accounts for small core vibrations because both centrifugal stretching and small vibrations reduce the energies of the high-spin band members. The use of a variable moment of inertia has improved the agreement between the calculated and experimental energies of high-spin members of rotational bands in the $A \sim 135$ and $A \sim 190$ regions, but usually did not alter the values of β and γ that were obtained with the model of Meyer-ter-Vehn.

C. Single particle plus core excitations

Several theoretical investigations of the low-lying states in the odd-mass $^{115-125}$Sb nuclei have been made in which these states are described as an odd proton coupled to various phonon vibrations of the even-mass Sn cores. The most complete of these studies is that by Vanden Berghe and Heyde,[12] in which the odd proton was allowed to occupy the $3s_{1/2}$, $2d_{5/2}$, $2d_{3/2}$, $1g_{7/2}$, and $1h_{11/2}$ shell-model orbitals and both quadrupole and octupole vibrations were included. A similar treatment was performed by Sen and Sinha[13] who obtained results consistent with those of Vanden Berghe and Heyde. Both of these studies achieved a good overall agreement with the experimental energy levels and electromagnetic properties of low-spin states below an excitation energy of 3 MeV. These calculations are also in agreement with the experimental spectroscopic factors obtained with the (^{3}He, d) reaction.[2] The $\frac{9}{2}^+$ states that were observed in the present work for each of the odd-mass Sb nuclei at about 1300 keV are interpreted as the $2d_{5/2}$ proton coupled to the first excited 2^+ phonon states in the corresponding $^{A-1}$Sn cores, which have comparable energies.

Although the low-spin states in Sn nuclei can be described as phonon vibrations, the high-spin states tend to be relatively pure two-neutron excitations because often there is only one unique high-spin configuration at a sufficiently low energy. This suggests that many high-spin states in odd-mass Sb nuclei can be described by two-neutron one-proton ($\nu^2\pi$) configurations. The lowest $\frac{15}{2}^{(-)}$ and $\frac{19}{2}^{(-)}$ levels observed in each of the Sb nuclei studied have energies that are consistent with the 5^- and 7^- $^{A-1}$Sn(ν^2) core excitations coupled to the $2d_{5/2}$ proton. The 2^+ phonon excitations coupled to the $1h_{11/2}$ proton are also expected to yield $\frac{15}{2}^-$ states at about 2600 keV; a second $\frac{15}{2}^{(-)}$ level in ^{115}Sb at 2638 keV suggests the presence of the two $\frac{15}{2}^-$ configurations near these excitations. The $\frac{21}{2}^{(-)}$ and $\frac{23}{2}^{(-)}$ levels observed in some of the Sb nuclei are believed to result from (ν^2) 7^--9^- excitations coupled to $\pi d_{5/2}$ or $\pi g_{7/2}$.

The $\frac{19}{2}^{(-)}$ level in ^{115}Sb was observed to be isomeric with a meanlife of $\tau = 230 \pm 4$ ns and measured to have a g factor of $+0.290 \pm 0.005$. Using empirical single-particle g factors along with additivity, the expected g factor for the ($\nu h_{11/2}, \nu d_{3/2}; 7^-$)($\pi d_{5/2}$) configuration is $g = +0.32$, which confirms the fact that this configuration is a dominant component of the ^{115}Sb $\frac{19}{2}^{(-)}$ level. Bron *et al.*[18] have deduced from the lifetime that the $E2$ strength between the isomeric $\frac{19}{2}^{(-)}$ level and the lowest $\frac{15}{2}^{(-)}$ level is enhanced by a factor of about 3 over that expected from the $7^- \rightarrow 5^-$ $E2$ strength in ^{114}Sn. This enhancement is explained by the admixtures of configurations involving the 2^+ and 4^+ core excitations coupled to the $1h_{11/2}$ proton.

The $\frac{25}{2}^{(+)}$ and $\frac{27}{2}^{(+)}$ levels observed in the odd-mass Sb nuclei are expected on the basis of the ($\nu h^2_{11/2}, 10^+$) excitation of the Sn cores coupled to the $2d_{5/2}$ and $1g_{7/2}$ protons, respectively. Previously, the 3130-keV $\frac{25}{2}^{(+)}$ isomer ($\tau = 340$ μs) in ^{117}Sb has been interpreted as having a ($\nu h^2_{11/2}, 10^+$) $\times$ ($\pi d_{5/2}$) configuration, which is consistent with the g factor of this state.[17] The $\frac{25}{2}^{(+)}$ state in ^{115}Sb lies ~530 keV higher in energy than in ^{117}Sb, which is consistent with the energy expected for this configuration on the basis of the energies of the ($\nu h^2_{11/2}, 10^+$) states of the Sn cores. Both from energy and lifetime considerations, it is also believed that the $(\frac{27}{2}^+)$ isomer ($\tau = 1.23$ s) observed in ^{119}Sb in the present experiment is the ($\nu h^2_{11/2}$, 10^+)($\pi g_{7/2}$) configuration. The fact that a ($\nu h^2_{11/2}$, 10^+)($\pi d_{5/2}$)$\frac{25}{2}^+$ isomer, observed in ^{117}Sb, is not seen in ^{119}Sb is reasonable since the $g_{7/2}$ orbital is becoming nearly degenerate in energy with the $d_{5/2}$ orbital in ^{119}Sb which can result in a $\frac{27}{2}^+$ state that is slightly lower in energy than the $\frac{25}{2}^+$ state. This would then explain the long lifetime which results from a converted low-energy $(\frac{27}{2}^+) \rightarrow \frac{21}{2}^{(-)}$ $E3$ transition.

V. SUMMARY

The nuclear structure of high-spin states has been investigated in ^{113,115,117,119}Sb by γ-ray measurements following ^{A}Cd(^{6}Li, $3n$)$^{A+3}$Sb reactions. Results of this investigation are summarized in Figs. 4–7. Systematic $\Delta J = 1$ bands built on low-

lying intruder $\frac{9}{2}^+$ states were observed in each of the Sb nuclei studied. These $\frac{9}{2}^+$ bandheads are believed to result from the excitation of a $1g_{9/2}$ proton across the $Z = 50$ closed shell. The observed properties of the $\Delta J = 1$ bands are consistent with significant prolate deformations. A deformation asymmetry of $\gamma = 20°$ is implied by the band spacings. The systematics of these $\frac{9}{2}^+$ states in the odd-mass Sb($Z = 51$) nuclei have been connected to proton-hole excitations of I($Z = 53$), Cs($Z = 55$), and La($Z = 57$) nuclei[23-25] of the $Z > 50$ transition region as well as to the 0_2^+ 2p-2h proton excitations in the even Sn nuclei.[47]

In addition to the collective bands, the (^{6}Li, $3n$) reactions populated the expected $\frac{5}{2}^+$, $\frac{7}{2}^+$, and $\frac{11}{2}^-$ single-particle states as well as a number of high-spin states consisting of single-particle coupled to Sn core excitations. The single-particle states involved the $2d_{5/2}$, $1g_{7/2}$, and $1h_{11/2}$ proton orbitals. The core excitations included both phonon vibrations and two-neutron states. Several isomers involving the latter were studied to determine their ($\nu^2\pi$) structure.

ACKNOWLEDGMENTS

We wish to thank Dr. K. Heyde and Dr. J. Meyer-ter-Vehn for private communications involving the theoretical interpretation of these results. We acknowledge several helpful communications with Professor H. Verheul regarding independent experimental results on related studies. Phil Moskowitz assisted with much of the experimentation and data analysis. This work was supported in part by the National Science Foundation.

*Present address: Brookhaven National Laboratory, Upton, New York 11973.
†Permanent address: Physics Dept., SUNY at Binghamton, New York 13901.
‡Permanent address: Universitat Konstanz, 7750 Konstanz, Germany.

[1]S. Raman and H. J. Kim, Nucl. Data. Sheets B5, 182 (1971); 16, 195 (1975); Nuclear Data Group, *Nuclear Data Sheets, 1959–1965* (Academic, New York, 1966), pp. 983 and 1005.
[2]M. Conjeaud, S. Harar, and Y. Cassagnou, Nucl. Phys. A117, 449 (1968).
[3]R. L. Auble, J. B. Ball, and C. C. Fulmer, Phys. Rev. 169, 955 (1968).
[4]M. Conjeaud, S. Harar, M. Caballero, and N. Cindro, Nucl. Phys. A215, 383 (1973).
[5]R. Kernell, H. J. Kim, R. L. Robinson, and C. H. Robinson, Nucl. Phys. A176, 449 (1971).
[6]A. D. Jackson, E. H. Rogers, and G. L. Garrett, Phys. Rev. 175, 65 (1968).
[7]J. A. Carr, K. Shafer, R. A. Warner, Wm. C. McHarris, and W. H. Kelly, Michigan State University Cyclotron Lab. Annual Reports 1974–1976, 1976 (unpublished); and to be published; W. H. Kelly, private communication.
[8]G. Berzins and W. H. Kelly, Nucl. Phys. A92, 65 (1967).
[9]R. Duffait, A. Charvet, and R. Chery, Z. Phys. A272, 315 (1975).
[10]A. Charvet, R. Chery, D. Huuphuoc, R. Duffait, and M. Morque, J. Phys. (Paris) 35, 805 (1974).
[11]M. E. J. Wigmans, R. J. Heynis, P. M. A. van der Kam, and H. Verheul, Phys. Rev. C 14, 243 (1976).
[12]G. VandenBerghe and K. Heyde, Nucl. Phys. A163, 478 (1971).
[13]S. Sen and B. K. Sinha, Nucl. Phys. A157, 497 (1970).
[14]A. K. Gaigalas, R. E. Shroy, G. Schatz, and D. B. Fossan, Phys. Rev. Lett. 35, 555 (1975).
[15]K. Heyde, M. Waroquier, H. Vincx, and P. Van Isacker, Phys. Lett. 64B, 135 (1976).
[16]P. Van Isacker, M. Waroquier, H. Vincx, and K. Heyde, Nucl. Phys. A292, 125 (1977).
[17]W. D. Fromm, H. F. Brickmann, F. Donau, C. Heiser, F. R. May, V. V. Pashkevitch, and H. Rotter, Nucl. Phys. A243, 9 (1975); C. Heiser, H. F. Brickmann, W. D. Fromm, and U. Hagemann, *ibid.* A145, 81 (1970).
[18]J. Bron, W. H. A. Hesselink, H. Bedt, H. Verheul, and G. VandenBerghe, Nucl. Phys. A279, 365 (1977).
[19]R. Kamermans, Tj. Ketel, and H. Verheul, Z. Phys. A279, 99 (1976).
[20]R. E. Shroy, A. K. Gaigalas, G. Schatz, and D. B. Fossan, Bull. Am. Phys. Soc. 20, 687 (1975); 19, 1029 (1974); 20, 1187 (1975).
[21]P. M. Swertka, T. P. Sjoreen, U. Garg, and D. B. Fossan, Bull. Am. Phys. Soc. 22, 1026 (1977).
[22]D. M. Gordon, M. Gai, A. K. Gaigalas, R. E. Shroy, and D. B. Fossan, Phys. Lett. 67B, 161 (1977).
[23]D. B. Fossan, M. Gai, A. K. Gaigalas, D. M. Gordon, R. E. Shroy, K. Heyde, M. Waroquier, H. Vincx, and P. Van Isacker, Phys. Rev. C 15, 1732 (1977); P. Chowdhury, P. M. Stwertka, A. Neskakis, U. Garg, T. P. Sjoreen, and D. B. Fossan, Bull. Am. Phys. Soc. 23, 555 (1978).
[24]U. Garg, T. P. Sjoreen, and D. B. Fossan, Phys. Rev. Lett. 40, 831 (1978).
[25]U. Garg, P. Chowdhury, T. P. Sjoreen, and D. B. Fossan, Bull. Am. Phys. Soc. 23, 90 (1978).
[26]D. B. Fossan, in Proceedings of the International Symposium on Nuclear Physics, Calcutta, 1977 (to be published).
[27]A. Bohr and B. Mottelson, *Nuclear Structure* (Benjamin, New York, 1975), Vol. II.
[28]F. S. Stephens, Rev. Mod. Phys. 47, 43 (1975).
[29]J. Meyer-ter-Vehn, Nucl. Phys. A249, 111 (1975); A249, 141 (1975).
[30]H. Toki and A. Faessler, Nucl. Phys. A253, 231 (1975).
[31]U. Hagemann and F. Donau, Phys. Lett. 59B, 321 (1975).
[32]G. Alaga and V. Paar, Phys. Lett. 61B, 129 (1976).
[33]A. Arima and F. Iachello, Phys. Rev. C 14, 761 (1976); M. Gai, D. Strottman, A. Arima, and F. Iachello (to be published).
[34]J. O. Newton, in *Nuclear Spectroscopy and Reactions*, edited by J. Cerny (Academic, New York, 1974), Chap. VII. E.
[35]See, for example, B. A. Brown, P. M. S. Lesser, and D. B. Fossan, Phys. Rev. C 13, 1900 (1976).
[36]R. E. Shroy, Ph.D. thesis, S.U.N.Y. at Stony Brook,

1976 (unpublished).
[37]J. Christiansen, H.-E. Mahnke, E. Recknagel, D. Reigel, G. Schatz, and G. Weyer, Phys. Rev. C 1, 613 (1970).
[38]R. E. Shroy, G. Schatz, and D. B. Fossan, Bull. Am. Phys. Soc. 19, 1001 (1974); Hyperfine Interactions 4, 738 (1978).
[39]F. D. Feoick and W. R. Johnson, Phys. Rev. 187, 39 (1967).
[40]T. E. Faber, *Introduction to the Theory of Liquid Metals* (Cambridge Univ. Press, London, 1972), p. 304; E. H. Hugh and T. P. Das, Phys. Rev. 143, 453 (1966).
[41]S. R. Faber, L. E. Young, and F. Bernthal, Bull. Am. Phys. Soc. 23, 355 (1978).
[42]H. Verheul, private communication.
[43]K. Nakai, Phys. Lett. 34B, 269 (1971).
[44]See, for example, A. de-Shalit and H. Feshbach, *Theoretical Nuclear Physics* (Wiley, New York, 1974), Vol. 1, p. 419.
[45]G. VandenBerghe and E. Degueck, Z. Phys. 262, 25 (1975).
[46]R. G. Markham, R. K. Bhowsrik, P. A. Smith, J. A. Nolan, and M. A. Shahabuddin, Bull. Am. Phys. Soc. 21, 634 (1976).
[47]J. Bron, W. H. A. Hesselink, L. K. Peker, A. van Poelgeest, J. Uitzinger, H. Verheul, and J. Zalmstra, in Contributions to the International Conference on Nuclear Structure, Tokyo, 1977 (to be published).
[48]A. S. Davydov and G. F. Filipov, Nucl. Phys. 8, 237 (1958).